THE EFFECT OF ENTRAINMENT ON DROPLET SPECTRUM EVOLUTION

by

V.A. Pissimanis

A thesis submitted to the Faculty of Graduate Studies and Research in partial fulfillment of the requirements for the degree of Master of Science

Department of Meteorology
McGill University
Montreal, Canada

August 1974

ABSTRACT

The effect on the growth of cloud droplets of entrainment of environmental air into the core of a growing convective cloud is investigated.

Entrainment with clear air, cloudy air (containing small droplets), and clear saturated air are considered. Starting from representative initial droplet distributions, of continental and maritime types of clouds, the droplet spectra develop experiencing entrainment, coalescence and condensation.

The results indicate that in both cases, when an entrainment rate parameter of 10^{-3} $\sec^{-1}$ is applied, the development is delayed by approximately 2 minutes, for clear air entrainment. For entrainment of cloudy air the delay is approximately 1 min.

Thus, from a point of view of time lag, entrainment does not retard the droplet spectrum evolution very much, particularly when the entrainment may be considered to take place with cloudy air.

RESUME

L'effet de l'entraînement de l'air environnement dans le noyeau d'un nuage convectif en plein développement sur la croissance des gouttelettes est étudié ici.

L'entraînement de l'air clair, de l'air nuageux (contenant de fines gouttelettes) et de l'air clair saturé est consideré. En partant de distributions initiales de gouttelettes représentatives des nuages à caractère continental et maritime, les spectres de gouttelettes se développent par entraînement, coalescence et condensation.

Les résultats pour l'entraînement de l'air clair indiquent que dans les deux cas, lorsqu'un taux d'entraînement de 10^{-3} sec^{-1} est appliqué, le développement est retardé d'environ 2 minutes. Pour l'entraînement de l'air nuageux, le retard est d'environ 1 minute.

Donc, du point de vue de décalage de temps, l'entraînement ne retarde pas beaucoup l'évolution du spectre des gouttelettes, et cela spécialement lorsque c'est de l'air nuageux qui subit l'entraînement.

ACKNOWLEDGEMENTS

This study was conducted under the supervision of Dr. H. Leighton, to whom I wish to express the deepest gratitude for his assistance and encouragement.

I am also indebted to Dr. R. Rogers, for his beneficial advice.

I wish to express my thanks to Miss P. Sharpe and Mr. A. Schwartz who often helped me with programming problems.

I am deeply grateful to Professor L.N. Carapiperis, Head of the Department of Meteorology of the University of Athens, who helped me and encouraged me to undertake graduate studies at McGill University.

I am also deeply grateful to the Greek Government for having provided a fellowship which made my two years study possible.

Appreciation is extended to Mrs. G. Sheldon who typed the manuscript, and to Mrs. S. Yip who prepared the drawings.

TABLE OF CONTENTS

	Page
ABSTRACT	i
RESUME	ii
ACKNOWLEDGEMENTS	iii
LIST OF FIGURES	v
1. INTRODUCTION	1
2. THEORY	8
2.1 Physical model	8
2.2 Magnitude of the entrainment rate parameter	9
2.3 Thermodynamic procedure	10
3. THE MODEL	14
3.1 General description of the model	14
3.2 Coalescence	17
3.3 Condensation	19
3.4 Initial distribution	20
4. PARTICULAR CASES AND RESULTS	22
4.1 Continental cloud case	22
4.2 Results	26
4.3 Maritime cloud cases	47
4.4 Results	51
4.5 Simulation of entrainment in the adiabatic case	60
5. SUMMARY	66
REFERENCES	70
APPENDICES	73
1. Computer program for the thermodynamic procedure	73
2. Cloud droplet growth model	79
3. Plotting program	91

LIST OF FIGURES

		Page
Fig. 2.1 :	Graphical representation of the thermodynamic procedure.	11
Fig. 3.1 :	Schematic diagram showing the procedure used in the computations.	16
Fig. 4.1 :	Initial droplet distribution for the continental cloud case.	23
Fig. 4.2 :	Temperature profiles, represented on a Tephigram, without entrainment and with entrainment with clear air ($R' = 10^{-3}$ sec^{-1} and 0.5×10^{-3} sec^{-1}), for the continental case.	25
Fig. 4.3 :	Liquid water content profiles, as a function of height, without entrainment and with entrainment with clear air ($R' = 10^{-3}$ sec^{-1} and 0.5×10^{-3} sec^{-1}), for the continental case.	28
Fig. 4.4 :	Temperature profiles, represented on a Tephigram, without entrainment and with entrainment with cloudy air ($R' = 10^{-3}$ sec^{-1} and 0.5×10^{-3} sec^{-1}), for the continental case.	29
Fig. 4.5 :	Liquid water content profiles, as a function of height, without entrainment and with entrainment with cloudy air ($R' = 10^{-3}$ sec^{-1} and 0.5×10^{-3} sec^{-1}), for the continental case.	30
Fig. 4.6 :	Liquid water content profiles, as a function of height, without entrainment, and with entrainment with clear, cloudy and saturated clear air ($R' = 10^{-3}$ sec^{-1}), for the continental case.	31
Fig. 4.7A :	Mass distribution after 0, 6, 9 and 11.5 min without entrainment, for the continental case.	33
Fig. 4.7B :	Mass distribution after 6, 9 and 11.5 min with entrainment with clear air ($R' = 10^{-3}$ sec^{-1}), for the continental case.	33
Fig. 4.8A :	Mass distribution after 6, 9 and 11.5 min with entrainment with clear air ($R' = 0.5 \times 10^{-3}$ sec^{-1}), for the continental case.	35

		Page
Fig. 4.8B :	Mass distributions at time t = 11.5 min without entrainment and with entrainment with clear air ($R' = 10^{-3}$ sec^{-1} and 0.5×10^{-3} sec^{-1}), for the continental case.	35
Fig. 4.9 :	Drop concentration, as a function of height, without entrainment and with entrainment with clear and cloudy air, for the continental case.	37
Fig. 4.10 :	The radius of the 100th largest drop m^{-3}, as a function of height, without entrainment and with entrainment with clear, cloudy and clear saturated air, for the continental case.	38
Fig. 4.11 :	The radar reflectivity factor, as a function of height, without entrainment and with entrainment with clear, cloudy and clear saturated air, for the continental case.	39
Fig. 4.12A:	Mass distribution after 6, 9 and 11.5 min with entrainment with cloudy air ($R' = 10^{-3}$ sec^{-1}), for the continental case.	41
Fig. 4.12B:	Mass distribution after 6, 9 and 11.5 min with entrainment with cloudy air ($R' = 0.5 \times 10^{-3}$ sec^{-1}), for the continental case.	41
Fig. 4.13A:	Mass distribution at time t = 11.5 min, without entrainment and with entrainment with cloudy air ($R' = 10^{-3}$ sec^{-1} and 0.5×10^{-3} sec^{-1}), for the continental case.	42
Fig. 4.13B:	Mass distribution at time t = 11.5 min, without entrainment and with entrainment with clear, cloudy and clear saturated air for $R' = 10^{-3}$ sec^{-1}, for the continental case.	42
Fig. 4.14 :	Mass distribution after 6, 9 and 11.5 min with entrainment with clear saturated air, for the continental case.	45
Fig. 4.15 :	Initial distribution for the maritime cases.	48
Fig. 4.16 : (A, B)	Temperature profiles, represented on a Tephigram, without entrainment and with entrainment with clear and cloudy air, for the maritime cases (I) and (II).	50

Page

Fig. 4.17 : Liquid water content profiles, as a function of height, without entrainment and with entrainment with clear and cloudy air, for the maritime case (I). 53

Fig. 4.18 : Liquid water content profiles, as a function of height, without entrainment and with entrainment with clear and cloudy air, for the maritime case (II). 54

Fig. 4.19 : Mass distribution after 0, 3, 6 and 9 min without entrainment, for the maritime case (I). 55

Fig. 4.20 : (A, B) Mass distributions at time t = 9 min, without entrainment and with entrainment with clear and cloudy air, for the maritime cases (I) and (II). 56

Fig. 4.21 : The radar reflectivity factor and the radius of the 100th largest drop m^{-3}, as a function of height, without entrainment and with entrainment with clear and cloudy air, for the maritime case (I). 57

Fig. 4.22 : Drop concentration, as a function of height, without entrainment and with entrainment with clear and cloudy air, for the maritime case (I). 59

Fig. 4.23 : The radar reflectivity factor and the radius of the 100th largest drop m^{-3}, as a function of height without entrainment and with entrainment with clear and cloudy air, for the maritime case (II). 61

Fig. 4.24 : Drop concentration, as a function of height, without entrainment and with entrainment with clear and cloudy air, for the maritime case (II). 62

Fig. 4.25 : (A, B) Mass distributions at time t = 11.5 min, representing simulation of entrainment with clear and cloudy air in the adiabatic case, for the conditions of continental case. 64

CHAPTER 1.

INTRODUCTION

One of the main factors that affects the development of a convective cloud is that the rising saturated air tends to be diluted by entraining some of the relatively dry environmental air. As the air in the environment is unsaturated, some of the liquid water in the rising parcel must be evaporated to maintain saturation in the cloudy air, as air from the environment is entrained.

Indeed many observations in small cumuli indicate that cloud temperatures are less than predictions from simple parcel theory, at different levels, and furthermore the liquid water content is only a fraction of the adiabatic value. Also rare observations on large thunderstorms indicate that entrainment of environmental air into the cloud takes place.

First Stommel (1947) presented a theory of convective clouds, the fundamental hypothesis being that the ascending current in a cloud entrains air from its surroundings. A method was developed for computing the 'mass flux' from the knowledge of the temperature and humidity inside and outside the cloud. The theory was applied to some observations of trade cumuli made near San Juan, Puerto Rico. He assumed arbitrarily unit 'mass flux' at the base of the cloud and he came to the result that the 'mass flux' roughly trebled over the cloud's depth, which ranged from 500 to 1500 m.

Since then, many researchers have dealt with the concept of 'entrainment' in cumulus clouds.

Byers and Hull (1949) measured the proportional rate of change of the area of triangles formed by balloons around thunderstorms to determine horizontal inflow or outflow of the air. They state that observations show outflow or horizontal divergence under the cloud base and convergence at all heights between about 4,000 and 23,000 feet, with divergence again in the uppermost levels. Also from these measurements they deduced the entrainment rate of environmental air.

Houghton and Cramer (1951) studied the problem of entrainment theoretically. On the basis of maintaining mass continuity, they derived equations for the rate of entrainment. They assume that a steady state exists, the cross section of the rising column is constant with height, the entrained air is uniformly mixed with the rising air, the environment is at rest, and finally that an ordered inflow occurs with no turbulent exchange between the environmental air and the rising column. This form of entrainment they called 'dynamic entrainment'. They determined the magnitude of the horizontal velocity-convergence, and they computed vertical velocities in the cloud. They suggested that their computational results tend to agree with previous observations made by Byers and Hull, (1949).

Malkus (1954) took measurements of temperature, vertical velocities, and water-vapor content of two clouds over the Caribbean Sea from a slow-flying instrumented aircraft. From these measurements numerous calculations were made, including 'dynamic entrainment' from the vertical velocity measurements, and 'gross entrainment' found by Stommel's method from the psychrograph records. She stated that the resulting values of the entrainment rate obtained by 'dynamic entrainment' were fairly consistent with those obtained by 'gross entrainment'.

Haltiner (1959), with calculations based on 'dynamic entrainment', extended the previous studies on convective currents to large cumulus clouds. He derived the value for a diffusion coefficient which applied to an upper-air sounding taken near the time and location of a thunderstorm. The model gave the right order of magnitude for the cloud height, vertical velocity, and temperature excess over the environment. He concluded also that cloud height, mass, vertical velocity, and liquid water content all increased with increasing a) initial temperature, b) environmental relative humidity and c) environmental lapse rate, but all decrease as the diffusion coefficient increases.

Squires and Turner (1962) presented a model based on a steady-state, turbulent, condensing plume, entraining environmental air according to the simple law that the inflow velocity at any height is proportional to the upward velocity of the plume. They derived the following equation for the conservation of mass, neglecting the difference in density between the updraft and the environment.

$$\frac{1}{M}\frac{dM}{dz} \approx \frac{2a}{b} = \frac{(\text{constant})}{b}$$

where: M is the mass flux in the jet

a is constant and represents the ratio of the inflow velocity to updraft speed. They take the value of a equal to 0.1

b is the radius of the plume or jet.

They presented with the use of this model a few calculations on cloud properties, such as range of updraft speed, liquid water content, and variation of radius with height, for deep cumuli. They suggested that the results were not inconsistent with the inadequate observational knowledge of these clouds.

This concept that the entrainment rate parameter, defined as the 'mass flux per unit distance', is inversely proportional to the ascending current has since been used often in models of cumulus clouds. (e.g. Danielsen et al (1972), Mason and Jonas (1974)).

Some laboratory experiments have been made to determine the value of the constant in the above formulation of the entrainment rate.

Experiments with bubbles were reported by Turner (1963). The results gave values of 2a between 0.54 and 0.75. Experiments to measure entrainment in jets (Ricou and Spalding (1961)) gave a value of the constant approximately equal to 0.2.

On the other hand from observations on emerging cumulus towers, Saunders (1961) found a value of 0.6 for this entrainment constant. Based on these measurements Mason and Jonas (1974) in their model of a non-precipitating cumulus cloud used the formula $\frac{1}{M}\frac{dM}{dz} = \frac{0.6}{b}$ for the entrainment rate parameter.

Recently Itier (1972) studied the validity of the above popular formula, on the basis of measurements of the diameter of cumulus towers and the maximum vertical velocities observed in four small clouds. He obtained the corresponding values of entrainment rate parameter. The results indicated that the entrainment rate parameter was related inversely to the radius of the tower. However, by comparison of two values of the entrainment rate parameter corresponding to the same tower radii but with different maximum vertical velocities, the larger entrainment rate parameter corresponded to the smaller maximum vertical velocity.

In addition to studies of entrainment much effort has been spent to investigate the general features of the droplet spectrum of cumulus clouds, and to describe its development with height by the condensation or coalescence mechanisms.

Warner (1969) examined a large number of droplet samples, in warm cumuli, and he found that bimodal distributions increase in frequency with height above cloud base and with increasing stability in the cloud environment.

On the other hand bimodal distributions were not confined to the cloud edges. He then suggested that the mixing at the growing cloud top determines the shape of the droplet spectrum.

The same author, (Warner (1970b)), examined lateral entrainment in a steady-state one-dimensional model. He suggested that such models cannot predict simultaneously values of liquid water content and cloud depth which are in agreement with observations.

He also, (Warner (1972)), examined the effect of mixing on the droplet spectrum in the first 300 m above cloud base, the spectrum developing by condensation only. He suggested that simple mixing between cloud and environment is unimportant in determining the drop size distribution, at least in the early stages of cloud growth.

Mason and Jonas (1974) created a model to simulate the real droplet spectra in small non-precipitating cumulus clouds, including mixing with the surroundings. They state that this model reproduces droplet spectra which closely resemble those measured by Warner (1969).

Other researchers (e.g. Árnason and Greenfield (1971), Nelson (1971), Silverman and Glass (1973)) created numerical models to simulate the real droplet spectra and the formation of rain in warm small cumuli.

On the other hand there are detailed models concerning deep convective clouds. For example, Danielsen's (1972) one-dimensional time-dependent numerical model, in which the emphasis is on hail growth, includes condensation with coalescence, sublimation, freezing, sedimentation, drop breakup, without disregarding the mixing term which modifies the vertical velocity, energy and water vapor of the ascending parcel.

From what has been stated up to here it is apparent that in the governing equations of a number of detailed and complicated models the mixing term is included, but emphasis has not been given to the single effect of entrainment on the droplet spectrum evolution.

For the purpose of describing precipitation development in the updraft region of a growing convective storm Leighton and Rogers (1974) created a model for droplet growth by condensation and coalescence in a strong non-entraining updraft.

By using this model an attempt is made in this study to discern the single effect of entrainment on the resulting droplet spectra. In other words, the cloud-droplet distribution evolves with time as a result of entrainment with its surroundings, condensation and coalescence. In particular the consideration of the problem is as follows.

We assume that a rising cloud parcel in the core of a growing convective cloud (large or small), entraining the stationary surrounding air changes its thermodynamic properties according to the basic thermodynamic equations. Then the development of the droplet spectrum by condensation and coalescence is determined by the above mentioned model (Leighton and Rogers (1974)), modified to include the effect of entrainment.

The way that the entrainment rate parameter has been chosen in this study is described in the next chapter. This parameter is kept constant with height. This assumption is equivalent to assuming that the radius of the cloud is uniform. While this simplifies the procedure, it is recognized that this is inconsistent with the assumption of a uniform vertical velocity, inherent in the Leighton and Rogers (1974) model.

Nevertheless a first estimate of the magnitude of entrainment of environmental air into the core of the cloud can be obtained.

CHAPTER 2.

THEORY

2.1 Physical Model

The mixing of environmental air into cloud is usually referred to as entrainment.

Let us assume a cloud core with a uniform constant updraft and consider in this core a rising parcel of air. If we assume that the upward velocity of the surroundings of the core of the cloud is much smaller than that of the parcel, the parcel will laterally entrain air from its surroundings.

The idealized procedure would be to divide the surroundings of the cloud core into a number of annular rings. Then the temperature, the upward velocity and the droplet mixing ratio would decrease as the distance from the core increases. In that case environmental clear air would be entrained to the outer annulus. The next inner annulus would entrain air from the outer annulus, acquiring thus a part of the clear air entrained to the outer annulus. This progressive procedure would continue and finally a portion of the environmental clear air will reach the core.

However, since it is not possible to determine the variation of the above mentioned properties inside the cloud, we proceed in a simpler way.

Basically we consider two regions. The core of the cloud with a uniform updraft and the environment having no vertical velocity. The difficulty lies in the choice of the appropriate environment.

As a first approximation the outside clear air is considered.

However as this gets entrained into the cloud, cloud condensation nuclei (CCN) will be activated. Since we are mainly interested in the development of the droplet spectrum, this factor may be important. So then we consider air with the same temperature of the environment but containing droplets. Finally as an intermediate assumption we calculated the effect of entrainment with saturated clear air.

Thus we consider three separate cases: entrainment into the cloud parcel in the updraft region (core) of clear unsaturated air, of saturated air not containing droplets, and of saturated air containing small droplets.

By definition if M represents the mass of a saturated cloud parcel which rises from a level z to a level z + dz entraining an amount of surrounding air dM, then the entrainment rate parameter is given by the formula: $R = \frac{1}{M}\frac{dM}{dz}$.

As was mentioned, in this study R is kept constant with height. We can also define the entrainment rate parameter per unit time, namely $R' = \frac{1}{M}\frac{dM}{dt}$, which is related to the previous one by the formula: $R' = R \cdot W$, where W represents the vertical velocity of the rising parcel. The units of R and R' are respectively $[cm^{-1}]$ and $[sec^{-1}]$.

2.2 Magnitude of the Entrainment Rate Parameter

In the introduction we referred to some of the observational and theoretical studies made on entrainment. The values of the entrainment rate parameter obtained may be summarized as follows:

a) Observational values.

Stommel (1947) and Malkus (1954) from investigations of small cumuli found the entrainment rate parameter to be of the order of 10^{-5} cm^{-1}. The same value has been obtained recently by B. Itier (1972) from observations of small convection towers.

Byers and Hull (1949) found values of the order of 10^{-6} cm^{-1} for large cumulonimbus clouds.

b) Theoretical values.

Houghton and Cramer (1951) derived an entrainment rate parameter of the order of 10^{-3} sec^{-1}, for clouds with depth about 1.6 km.

Haltiner (1959), for large cumuli, found R to be of the order of 10^{-6} cm^{-1}.

For our purpose the choice of the value of this parameter is made by taking into account on the one hand the range in which the observational and theoretical values are found, and on the other hand the formulation of Squires and Turner (1962), assuming an effective radius of the cloud core.

These considerations led to the adoption of the following values. For the continental type of cloud two values were used, namely $R = 10^{-6}$ cm^{-1} (10^{-3} sec^{-1}), and $R = 0.5 \times 10^{-6}$ cm^{-1} (0.5×10^{-3} sec^{-1}) with the vertical velocity taken to be 10 m sec^{-1}. For the maritime type of cloud one value is considered that is four times greater than in the previous case, i.e. $R = 4 \times 10^{-6}$ cm^{-1} (10^{-3} sec^{-1}) with the vertical velocity kept constant at 2.5 m sec^{-1}.

The above values are consistent with those that have been observed or theoretically computed for the appropriate size of clouds.

2.3 Thermodynamic Procedure

A graphical representation of this procedure is shown on a Tephigram in Fig. 2.1.

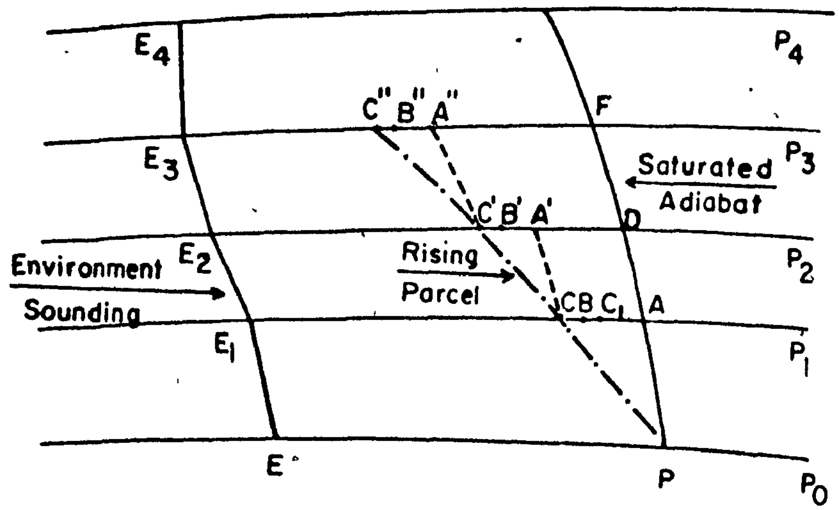

Fig. 2.1 Graphical representation of the thermodynamic procedure.

Point A : represents the cloud parcel at some pressure level P_1 at which mixing with the environment air is to take place.

Point B : represents the mixture (after isobaric mixing in a proportion R).

Point C : represents the final position of the parcel after saturation of the unsaturated mixture by isobaric evaporation (wet-bulb process).

Point C_1: represents the final position of the parcel after isobaric condensation in the case of mixing with saturated air.

The curve PADF represents the saturated adiabat from the point P, while CA', C'A" are the saturated adiabats through the points, C, C' respectively.

Without entrainment the rising parcel would follow the saturated adiabat PADF, assuming that P is the starting point of the calculations. However mixing at level P_1 with environment E_1 leads to the point B, and finally saturation by the wet-bulb process to the point C.

Continuing its ascent without entrainment the rising parcel would follow the saturated adiabat CA'. But mixing at level P_2 with environment E_2, leads finally to the point C'.

Thus as a result of progressive entrainment processes with clear air, the curve CC' represents the P-T curve of the rising cloud parcel instead of the saturated adiabat AD. In the case of mixing with saturated or cloudy air the resulting curve would be to the right of CC', between the same pressure levels P_1, P_2.

The process applied to the entire sounding gives the Pressure-Temperature profile of the rising cloud parcel of air taking into account entrainment of environmental clear air, namely curve PCC'C"... Correspondingly we would get to the right of this curve the P-T profile of the rising cloud parcel of air taking into account entrainment with saturated or cloudy air, in the same proportion R.

As far as the liquid water content of the parcel is concerned it changes at each time step as follows.

Let us consider that at pressure level P_o the cloud parcel contains L_o grams liquid water per gram of air. If the properties of the parcel are represented by C when it has risen to level P_1 it will contain an amount L_1 (gm/gm) which can be expressed as follows:

$L_1 = L_o$ + (condensation due to expansion)-

- (dilution due to mixing) -

- (evaporation by the wet-bulb process)

If the properties of the parcel are represented by C_1 when it has risen to the same level P_1, (in the case of entrainment with saturated or cloudy air), it will contain an amount L_1' (gm/gm) which can be expressed as follows:

$$\begin{aligned} L_1' = L_o &+ (\text{condensation due to expansion}) - \\ &- (\text{dilution due to mixing}) + \\ &+ (\text{condensation by the wet-bulb process}). \end{aligned}$$

This process applied to the entire path gives the liquid water content profile of the rising cloud parcel of air.

When entrainment with cloudy air takes place, the cloudy air which is considered to be mixed into the cloud core is assumed to have the temperature of the environment and a liquid water mixing ratio equal to the initial value of the rising cloud parcel in the updraft region. This is because the edges of the cloud are assumed to contain less liquid water content than the core region, as some measurements indicate (e.g. Zaitsev (1950)).

The liquid water content of the rising cloud parcel resulting from mixing in both cases is less than that which is predicted by simple parcel theory.

A numerical procedure following the three processes, namely adiabatic ascent, isobaric mixing, wet-bulb process, calculates the temperature, liquid water content, mixing ratio, and density of the rising cloud parcel of air at each step. A listing of the computer program used for these calculations is included in Appendix 1.

So from what has been stated up to here the calculations of the thermodynamic properties of the rising cloud parcel, which is experiencing entrainment may be made.

CHAPTER 3.

THE MODEL

3.1 General Description of the Model

The model determines the development of a droplet spectrum by condensation and coalescence. Growth by coalescence is determined by solving the stochastic collection equation, and growth by condensation is calculated from the diffusion equation.

When a saturated adiabatic process is assumed, the temperature decreases at the pseudoadiabatic rate and the amount of condensed water at any altitude is given by the adiabatic liquid water content. In the case that entrainment is considered the temperature decreases according to the P-T profile calculated from the thermodynamic procedure, described in the previous chapter. Also the liquid water content at each step is defined from the same procedure.

The liquid water content of the developing droplet spectrum experiences the following changes: a) It decreases due to entrainment at each time step, at a rate determined by the value of the parameter R. b) It increases by condensation, not necessarily at each time step as will be seen in the appropriate section. But, if condensation takes place, an appropriate amount of water is condensed, such that the liquid water content contained in the distribution diluted by entrainment is approximately equal to the value given at this level by the procedure described in the previous chapter.

The number of droplets per unit mass of air also changes due to the entrainment process, and as a result of collection. It is predominantly the small droplets in the spectrum that grow by condensation. However when entrainment with cloudy air takes place they are replenished, since at each step entrainment in a proportion R between the developing spectrum and the initial one is considered. A brief description of the numerical procedure is given schematically in Fig. 3.1. A listing of the computer program is included in Appendix 2.

The cloud droplets fall relative to each other with their terminal velocities, but do not leave the parcel. This assumption is reasonable provided that their terminal velocities are small compared to the updraft velocity.

However, the updraft velocity assumed in the maritime case, i.e. 2.5 m sec^{-1}, does not allow one to neglect the droplet fallout toward the end of the calculations. Nevertheless, since in order to evaluate the effect of entrainment a comparison is done between the spectra obtained with and without entrainment, this effect is counterbalanced assuming that in both cases it is approximately the same.

The initial parameters specified are the temperature and the pressure at the cloud base, the initial droplet spectrum, the environment properties and the updraft speed. The equations describing the condensation and coalescence process, that will be described in the next section, are integrated to give the development of the spectrum as a function of height. The time-step is always taken as 1 sec. This time interval has been found sufficiently small at least for the coalescence process (Leighton and Rogers (1974)).

The governing equations by which Leighton and Rogers modelled droplet growth by condensation and coalescence are described below briefly.

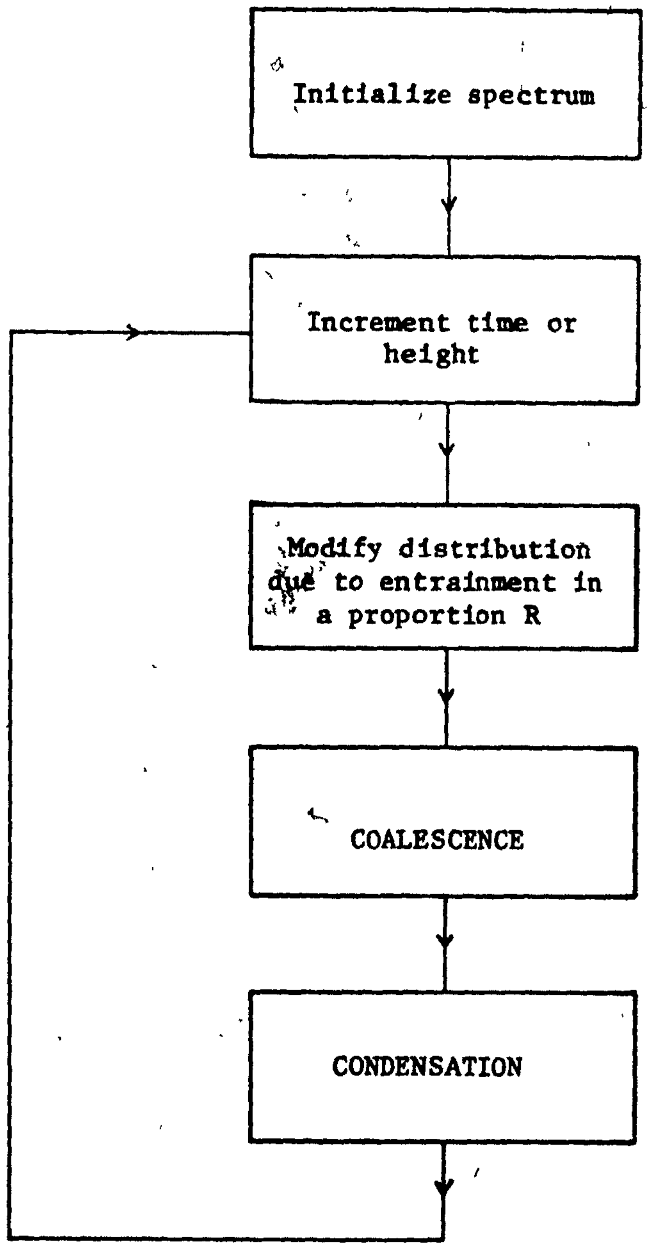

Fig. 3.1 Schematic diagram showing the procedure used in the computations.

3.2 Coalescence

The coalescence problem is solved by using the stochastic coalescence equation.

If $N(x)$ is a density function defined such that $N(x)dx$ is the concentration of droplets of mass x to $x + dx$ per unit volume of air, then the stochastic equation describing the rate of change of $N(x)$ is given by:

$$\frac{\partial N(x)}{\partial t} = \int_0^{x/2} dx' \; N(x_c) \; V(x_c, x') \; N(x') - \int_0^{\infty} dx' \; N(x) \; V(x, x') \; N(x') \quad , (1)$$

where $V(x,x')$ is the collection kernel, defined as the rate at which, the volume within which a droplet of mass x' will be captured, is swept out by a droplet of mass x. The collection kernel is related to the linear collision efficiency Y_c used by Shafrir and Neiburger (1963) as follows:

$$V(r/r_s) = \pi r^2 \cdot Y_c \; (r/r_s)^2 \quad \Delta v(r, r_s)$$

where r; (r_s) is the radius of the larger (smaller) droplet, and Δv the difference in velocities. Also $x_c = x - x'$.

The first term in equation (1), named gain integral, is the rate of change of $N(x)$ due to collisions between pair of droplets whose masses add to form x - mass droplets.

The second term, named loss integral, represents the number of droplets of mass x that are lost by collection with other droplets.

According to Berry's (1967) procedure x may be represented on a log scale by means of the transformation;

$$x(J) = x_o \exp \; [\; 3(J - 1)/J_o \;] \; .$$

where x_o is the smallest mass considered, and J_o an adjustable scale factor. A mass density function, $M(x)$, is defined by $M(x) = x\,N(x)$ where $M(x)dx$ is the mass of the drops per unit volume cloudy air, in the interval dx. In terms of J, the mass density function becomes

$$g(J) = M(x)\frac{dx}{dJ} = x\,N(x)\,\frac{3x}{J_o} . \qquad (2)$$

Introducing a log-increment density function $g_L(r)$, defined by $g_L(r)d\ln r = g(J)dJ$, we get $g_L(r) = 3x^2 N(x)$. Equation (2) can be used to write the collection equation (1) in the form

$$\frac{\partial g(J)}{\partial t} = x(J)\left\{\int_1^{J_d} \frac{x(J)}{x(J_c)}\, g(J_c)\, W(J_c, J')\, g(J')\, dJ' - \int_1^{\infty} g(J)\, W(J,J')\, g(J')\, dJ'\right\}. \qquad (3)$$

where: J_c is defined by $x_c = x_o \exp[3(J_c - 1)/J_o]$ and J_d by $x(J)/2 = x_o \exp[3(J_d - 1)/J_o]$. $W(J,J')$ is the modified collection kernel related to $V(x,x')$ by

$$W(J,J') = V[x(J),x(J')]/[x(J)\,x(J')] .$$

The smallest mass value is $x_o = 2.58 \times 10^{-10}$ g, the constant $J_o = 12/\ln 2$, and the parameter J takes values from 1 to 81. Therefore the range of radii is from 3.94 μm to 400 μm, doubling every 12 values of J.

The values of the fall velocities were taken from Stokes' law for radii smaller than 25 μm, and from Beard and Pruppacher's (1969) measurements for larger radii.

Collision efficiencies were taken in the model, from the compilation of values given by Mason (1973) for pairs of drops with radii larger than 30 μm, and were interpolated from Hocking and Jonas (1970) for pairs in which both droplets had radii less than or equal to 30 μm.

3.3 Condensation

The condensation problem in the model, is solved by the diffusional growth equation:

$$\frac{dr}{dt} = \frac{c}{r} \qquad (4)$$

where

$$c = (S - 1)\left[\frac{L^2\rho_L}{K\,R_v T^2} + \frac{R_v T\rho_L}{De_s(T)}\right]^{-1} \qquad (5)$$

with S the saturation ratio

L the latent heat of vaporization

ρ_L the density of water

R_v the gas constant for water

T the temperature

K the coefficient of thermal conductivity of air

D the diffusion coefficient of water vapor in air

$e_s(T)$ the equilibrium vapor pressure.

If $n(r,t)\,dr$ represents the number of droplets per unit volume of air with radii r to r + dr at time t, then at time t + Δt the spectrum will have developed by condensation only, to the form:

$$n(r, t + \Delta t) = \frac{r}{(r^2 - 2c\Delta t)^{1/2}}\, n(\sqrt{r^2 - 2c\Delta t}, t)\, \frac{\rho(t + \Delta t)}{\rho(t)} \qquad (6)$$

This solution is a special case of the general solution formulated by Kovetz (1969), using equation (4), where ρ(t) represents the density of the air at time t.

In terms of the 'mass distribution function' equation (6) becomes:

$$g\,[J(r),\, t + \Delta t] = \frac{r^5}{(r^2 - 2c\Delta t)^{5/2}}\, g\,[J(\sqrt{r^2 - 2c\Delta t}),\, t]\;\; \frac{\rho(t + \Delta t)}{\rho(t)} \quad . (7)$$

In the calculations the model determines the constant c not from the thermodynamic relation (5), but for a given time step the correct value of c is chosen as the one for which the liquid water content, obtained by integrating equation (7), corresponds most closely to the adiabatic value. In the case that entrainment takes place, the correct value of c is chosen as the one for which the liquid water content obtained by integration of the mass distribution, corresponds most closely to the liquid water content computed from the thermodynamic procedure at the corresponding level, taking into account entrainment.

However, at each time step several values of c are considered, each of which allows the minimum radius to correspond to an integral value of J. Consequently condensation does not take place at every time step, and the resulting numerical values of liquid water content oscillate about the analytically calculated ones.

3.4 Initial distribution

It is known from observations that cloud-droplet size distributions are generally asymmetrical with a tail extending towards the larger radii (Squires (1956), Diem (1948)). There has also been found a distinction between continental and maritime distributions near cloud base. Continental cumuli have narrow spectra with median droplet diameters, about 10 μm, and high concentration, while maritime cumuli have rather broad spectra with median droplet diameters, about 30 μm, and low concentration (Battan and Reitan (1957), Squires (1958a)).

The initial distributions used in the model are of the form defined by Scott (1968). He defined a dimensionless number density function by

$$\phi\ (s) = \frac{(\nu + 1)^{\nu+1}\ s^{\nu}\ e^{-s(\nu+1)}}{\Gamma(\nu + 1)} \qquad (8)$$

where $s = \frac{x}{\bar{x}}$, and ν is a measure of the width of the spectrum.

In terms of the 'mass density function' according to Berry's transformation formula equation (8) becomes

$$g(J) = \frac{3N_o}{J_o} \cdot \frac{(\nu + 1)^{\nu+1}}{\Gamma(\nu + 1)} \cdot \frac{x^{\nu+2}}{\bar{x}^{\nu+1}} \cdot \exp[- \frac{x}{\bar{x}} (\nu + 1)] \qquad (9)$$

where N_o is the total number of drops per unit volume.

$\bar{x}$ is the mean mass of the distribution

ν is a measure of the spectrum width, the relative variance of $N(x)$ being $(\nu + 1)^{-1}$.

Equation (9) contains three degrees of freedom, namely N_o, ν, $\bar{x}$.

In the present study these parameters are changed depending on whether the continental or maritime case is considered.

CHAPTER 4.

PARTICULAR CASES AND RESULTS

4.1 Continental Cloud Case

Initial Distribution

For the continental cloud the values of the parameters used in equation (9) were as follows:

N_o (cm^{-3})	$\bar{r}$ (μm)	$\tilde{\nu}$
900	8	3

The mass that corresponds to the above mean radius is $\bar{x} = 2.15 \times 10^{-9}$ g . The value of ν determines the width of the spectrum. For the above values of ν and $\bar{r}$ the resulting dispersion of the distribution of the 'number of droplets' is approximately 0.2. Also the above values of $\bar{x}$ and N_o result in a liquid water content equal to 1.9 g m^{-3}. Fig. 4.1 shows the initial distribution in terms of the 'number density distribution' in linear coordinates.

Initial Conditions

The initial conditions which are used to determine the pseudo-adiabatic ascent and the effect of entrainment on the temperature and liquid water content profile, are as follows:

The cloud base is taken at 825 mb (1703 m MSL) with a temperature of 13.5°C. These conditions refer to a particular storm day in Alberta (11/07/70) as described by English (1973). The cloud base height was measured from cloud photographs while the cloud base temperature was measured by aircraft. The updraft is assumed to be constant at 10 m sec^{-1}.

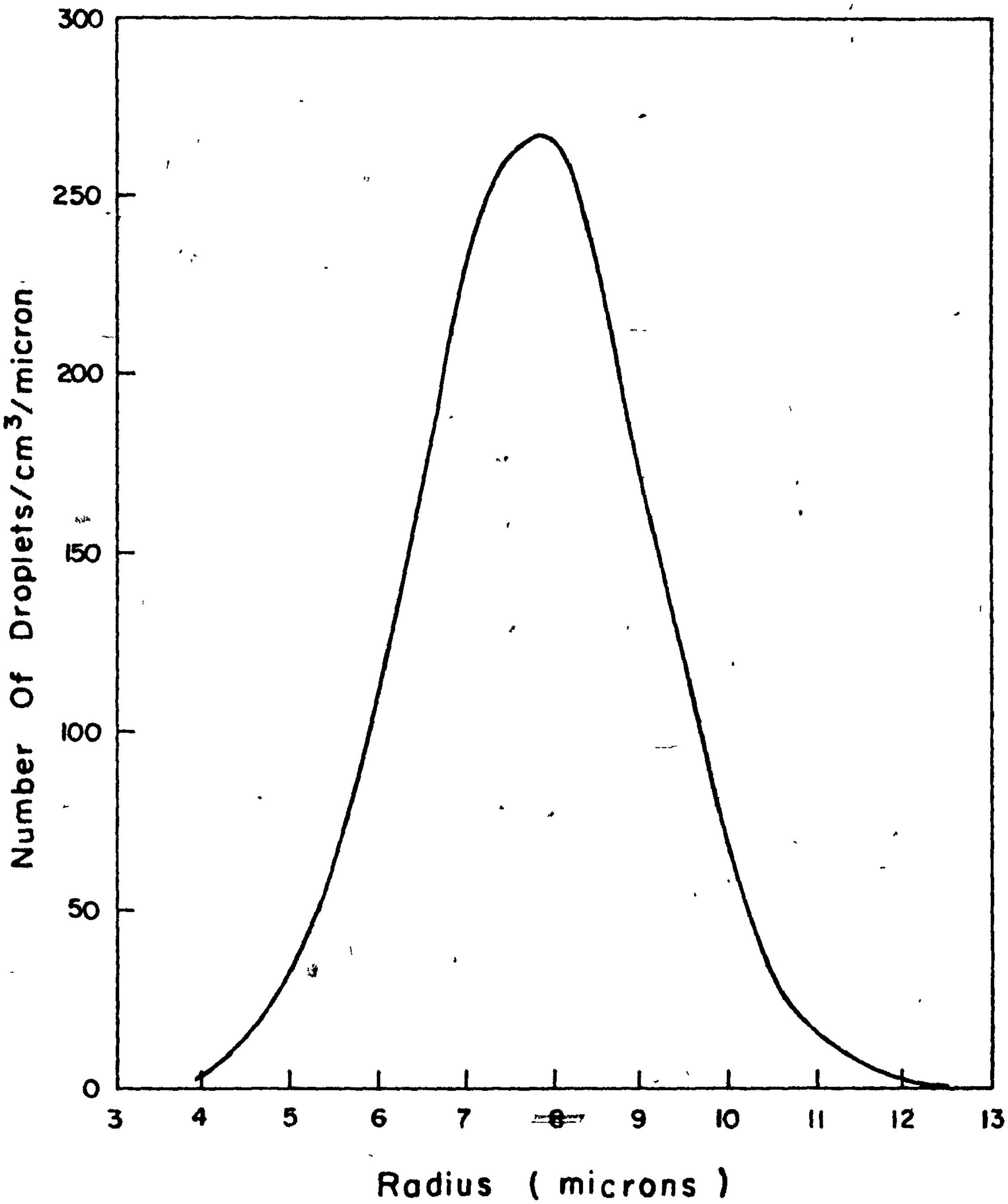

Fig. 4.1: Initial droplet distribution for the continental case.

Measurements of tower tops by photography indicate speeds of 13 m sec^{-1} to 20 m sec^{-1}. However the value of 10 m sec^{-1} is reasonable since it is kept constant along the whole path and therefore it could be accepted as an estimate of the mean value.

As far as the entrainment rate parameter is concerned, the computations are carried out for values or R' equal to 10^{-3} sec^{-1} and 0.5×10^{-3} sec^{-1} .

The whole procedure started 1005 m above cloud base where the adiabatic liquid water content was equal to the water content contained in the initial droplet spectrum, i.e. 1.9 g m^{-3}. It was stopped when the temperature of the pseudoadiabatically rising cloud parcel (i.e. no mixing) reached -40°C, which occurred after approximately 11.5 min. However when entrainment takes place the temperature of the rising cloud parcel becomes somewhat colder than -40°C. In addition in the last time steps the cloud parcel becomes colder than the environment, but it is still assumed that it rises with a constant velocity.

Environmental Conditions

Temperature and dew point soundings are also given by English (1973) for this particular day. Fig. 4.2 shows the environmental conditions and the adiabatic parcel temperature.

With the above conditions we proceeded in the examination of the effect of entrainment on the droplet spectrum evolution as follows:

a) Assuming that the cloud parcel ascends pseudoadiabatically we compute its thermodynamic properties, namely the temperature and the adiabatic liquid water content profiles. Then with the help of the model,

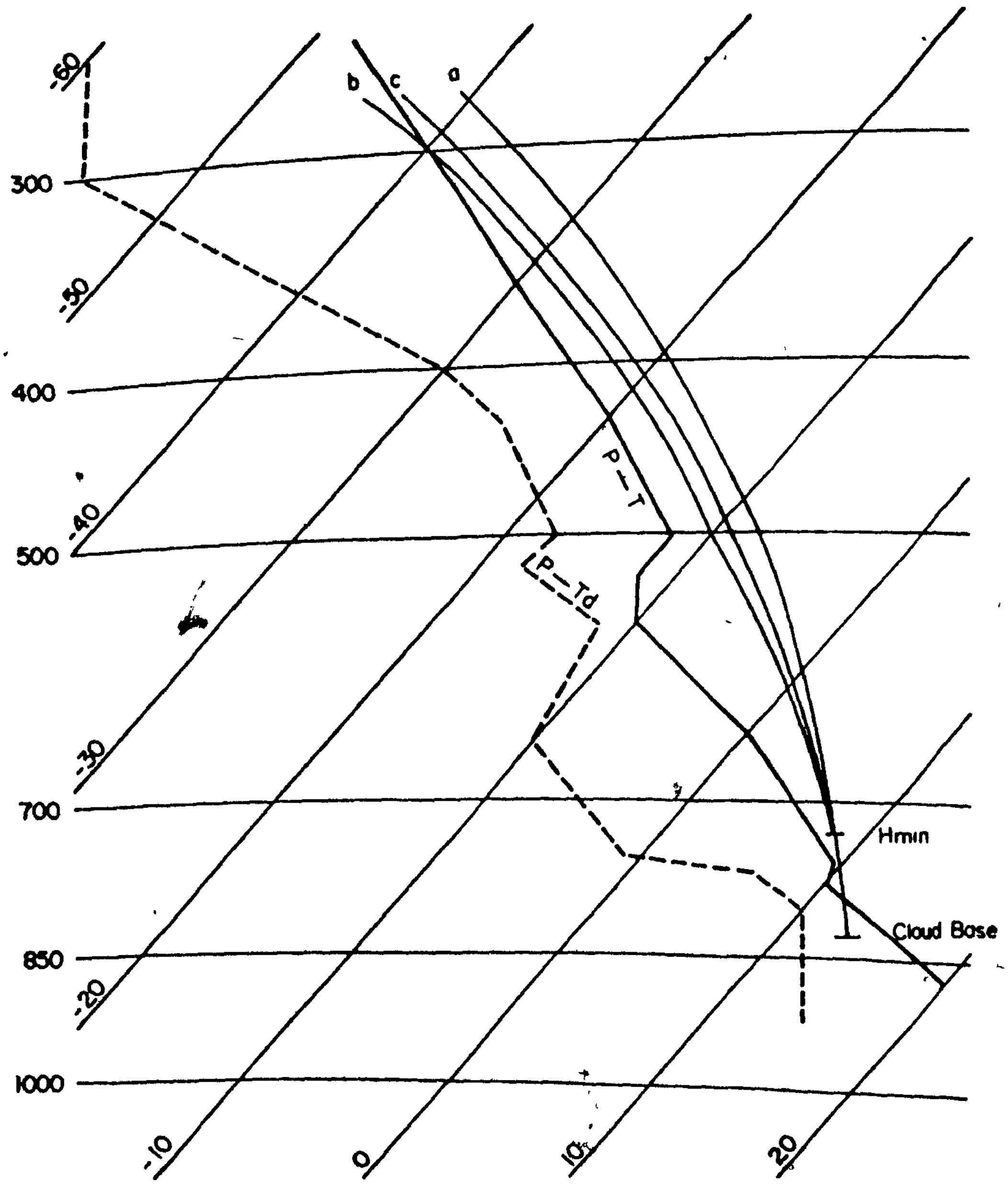

Fig. 4.2: Environmental and initial conditions for the continental case.

a) Temperature profile without entrainment
b) and c) Temperature profiles with entrainment with clear air, for values of $R' = 10^{-3}$ sec^{-1} and 0.5×10^{-3} sec^{-1} respectively.

described in the previous chapter, we determine the evolution of the droplet spectrum as a function of height.

b) The above procedure is repeated but assuming that the rising parcel entrains clear air at rates given by $R' = 10^{-3}$ sec^{-1} and 0.5×10^{-3} sec^{-1} . In this case also with the help of the 'thermodynamic procedure', the thermodynamic properties of the rising cloud parcel were found while with the help of the droplet growth model the droplet spectra were obtained.

c) The procedure is repeated for the same entrainment rates but assuming that the entrained air contains cloud droplets. The droplet spectrum is assumed to be the same as the initial droplet spectrum except that the droplet concentration has been reduced owing to the decrease in density.

d) Finally the procedure is repeated for entrainment of saturated but clear air at an entrainment rate of 10^{-3} sec^{-1} .

A comparison of the droplet spectra which are obtained in the last three cases to that obtained in the first case, at a certain time, indicates the effect of entrainment. The consideration of common values of the entrainment rate parameter in the three last cases allows a comparison among their resulting droplet spectra.

4.2 Results

Effect of Entrainment on the Thermodynamic Properties of the Cloud

In the following the effect of entrainment of environmental air on the thermodynamic properties of the core will be described.

Fig. 4.2 shows the deviations of calculated temperatures from those predicted by parcel theory, as a function of height (time), when entrainment takes place with clear environmental air, for both values of the entrainment rate parameter, i.e. $R' = 10^{-3}\ sec^{-1}$ and $R' = 0.5 \times 10^{-3}\ sec^{-1}$.

In addition Fig. 4.3 shows the deviations of the liquid water content from the adiabatic values, as a function of height (time), also when entrainment takes place with clear environmental air, for the above values of the parameter R' .

So as the entrainment with clear air increases the temperature and the liquid water content of the parcel decrease.

Figures 4.4 and 4.5 show respectively the temperature and liquid water content deviations from those predicted by parcel theory in the case that entrainment is considered to take place with cloudy air, for the same values of the entrainment rate parameter.

In this case also as the entrainment increases both the temperature and liquid water content of the parcel decrease.

A comparison between the case of the entrainment with clear air with that with cloudy air assuming a common entrainment rate parameter, (i.e. $10^{-3}\ sec^{-1}$), leads to the following conclusion.

Entrainment with cloudy air reduces the temperature and liquid water content at a significantly slower rate than entrainment with clear air. Consequently a large amount of entrainment with cloudy air may result in a smaller decrease in cloud temperature and liquid water content than a smaller amount of entrainment with clear air.

Fig. 4.6 is a plot of the liquid water content profiles in the adiabatic case together with the cases of entrainment with clear and cloudy air, for $R' = 10^{-3}\ sec^{-1}$. It is apparent that when entrainment with clear air takes place the value of liquid water content resulting

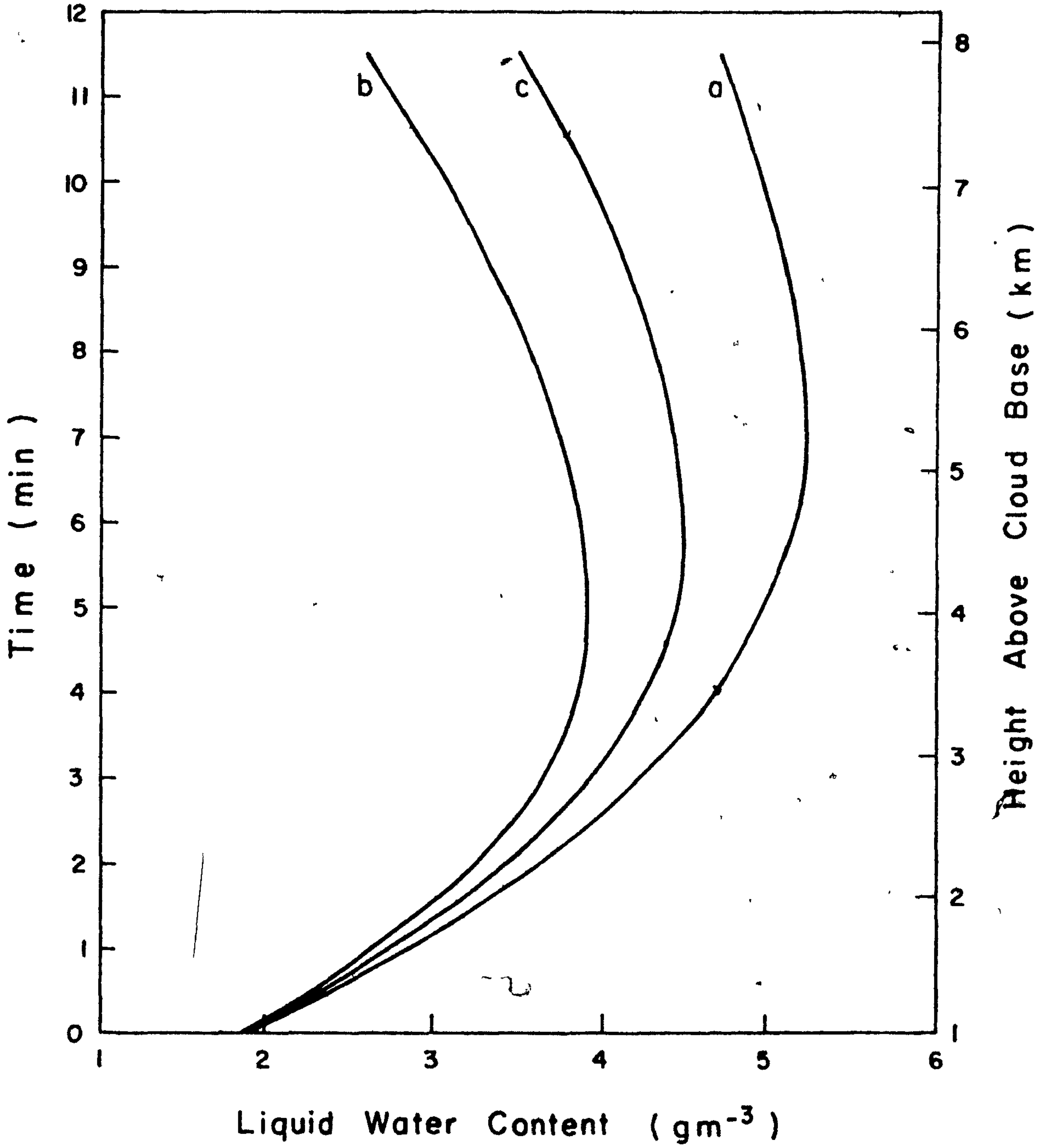

Fig. 4.3: Liquid water content profiles, as a function of height, for the continental case.

a) No entrainment.
b) and c) Entrainment with clear air, for values of $R = 10^{-3}$ sec^{-1} and 0.5×10^{-3} sec^{-1} respectively.

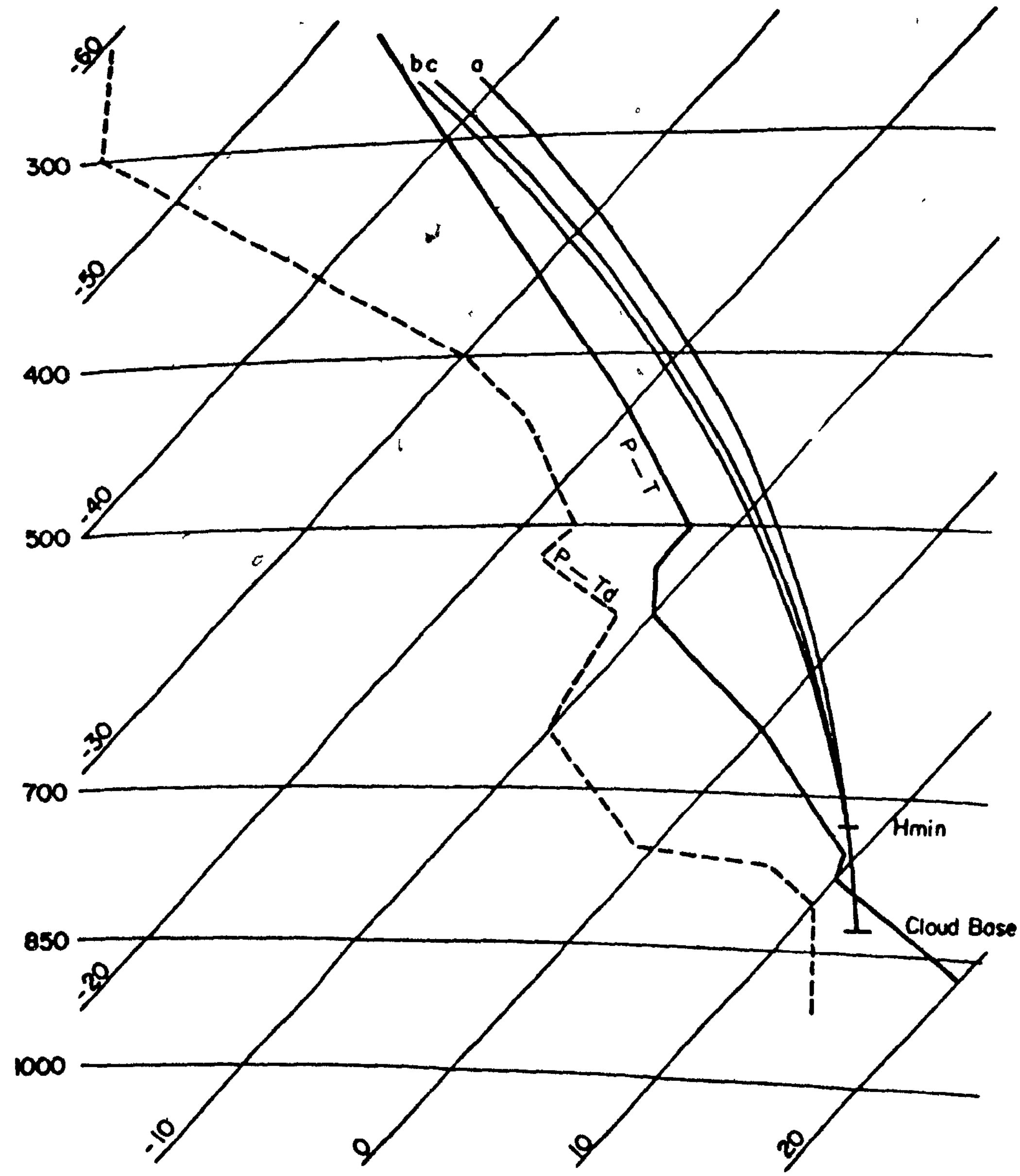

Fig. 4.4: Temperature profiles for the continental case.

a) No entrainment
b) and c) Entrainment with cloudy air, for values of R = 10^{-3} sec^{-1} and 0.5 x 10^{-3} sec^{-1} respectively.

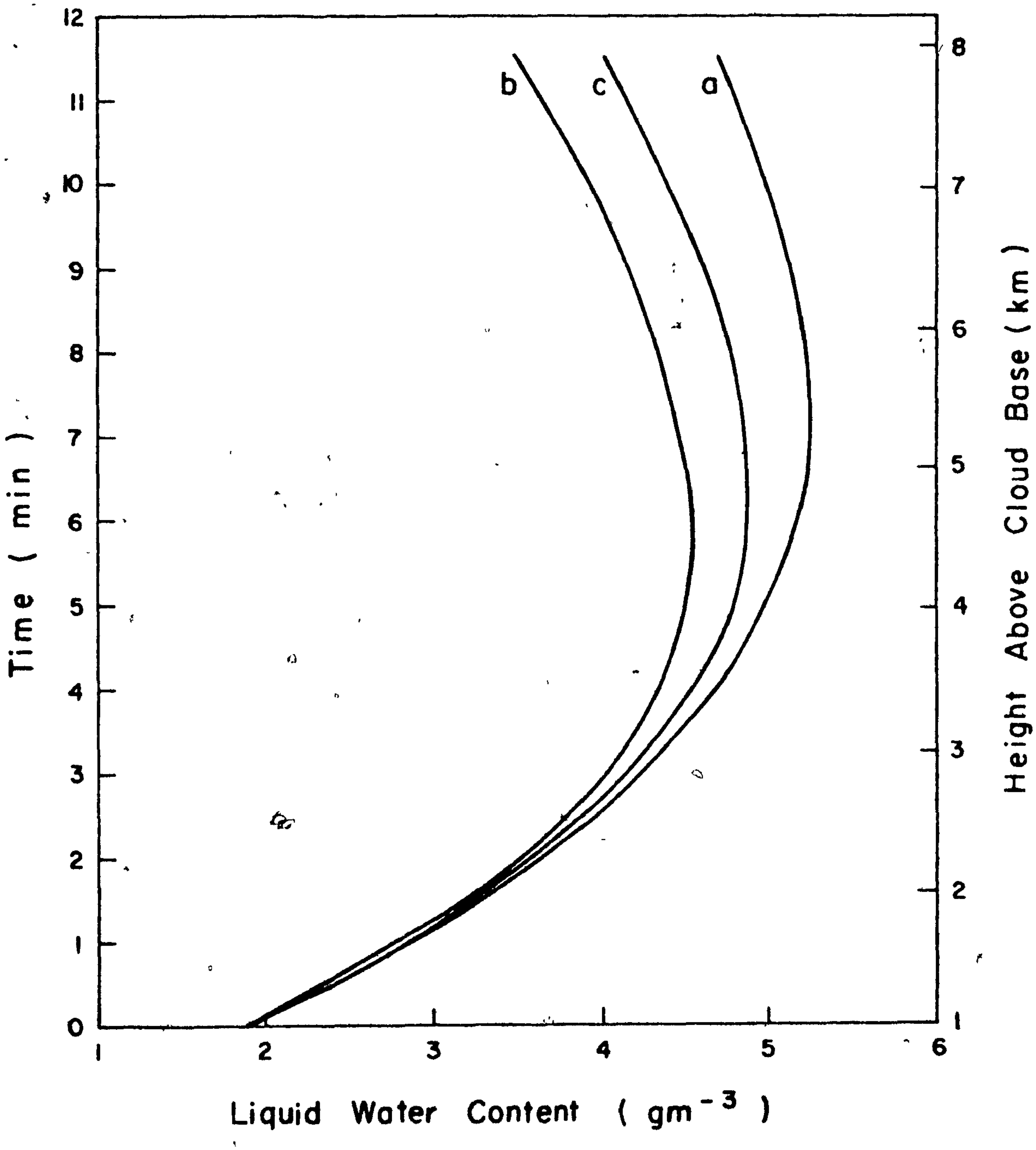

Fig. 4.5: Liquid water content profiles, as a function of height, for the continental case

a) No entrainment
b) and c) Entrainment with cloudy air, for values of $R' = 10^{-3}$ sec^{-1} and 0.5×10^{-3} sec^{-1} respectively.

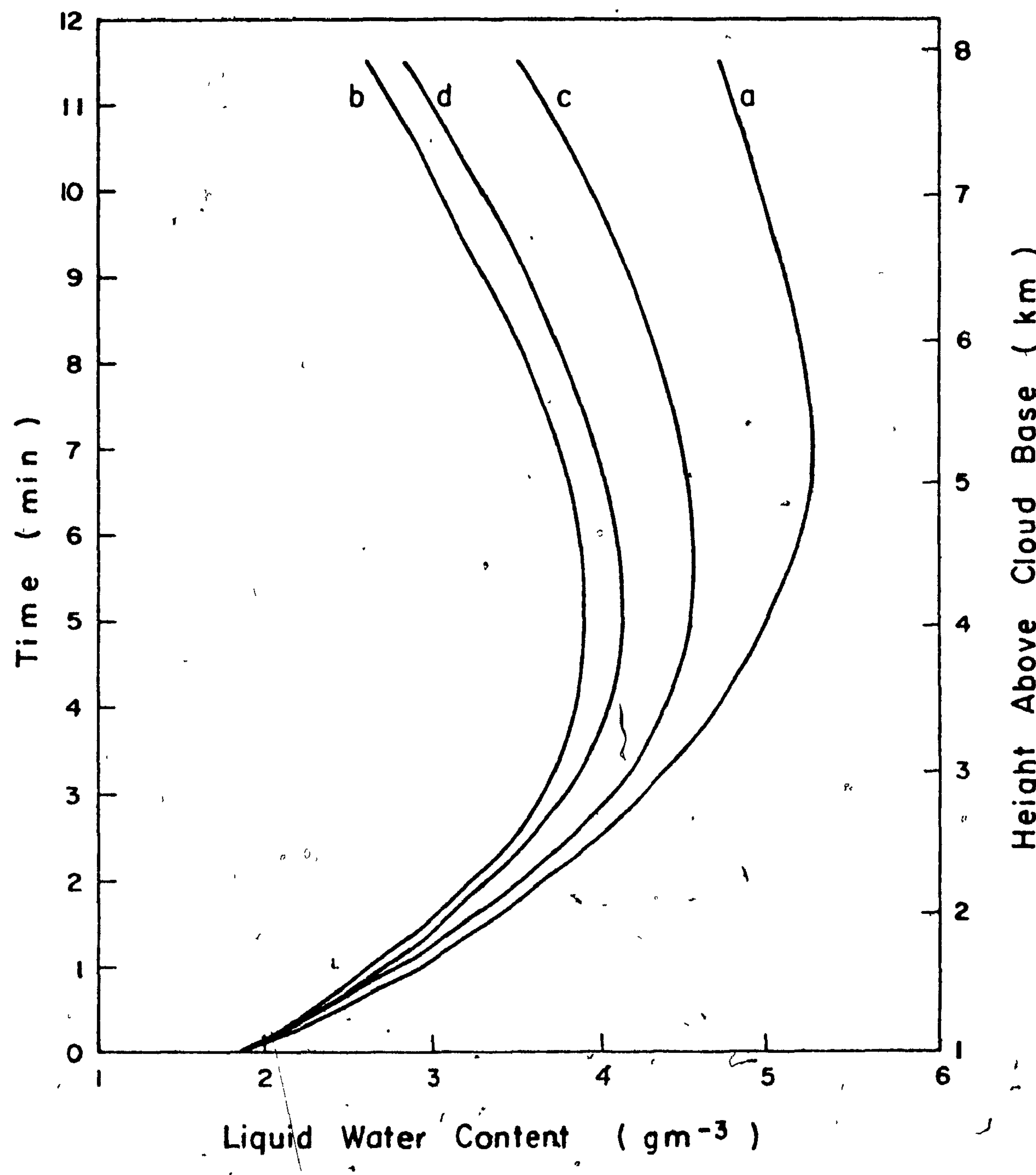

Fig. 4.6: Liquid water content profiles, as a function of height, for the continental case.

a) No entrainment
b) Entrainment with clear air, for $R' = 10^{-3}$ sec^{-1}
c) Entrainment with cloudy air, for $R' = 10^{-3}$ sec^{-1}
d) Entrainment with clear saturated air, for $R' = 10^{-3}$ sec^{-1}.

from the thermodynamic procedure after 11.5 min corresponds to 0.55 of the adiabatic value at this time, while in the case of entrainment with cloudy air, assuming the same R', the ratio of the corresponding values is 0.74.

As has been mentioned entrainment with saturated clear air is also examined, assuming one value of the entrainment rate parameter, namely $R' = 10^{-3}\ \text{sec}^{-1}$.

In this case the temperature profile on the Tephigram coincides with the one corresponding to entrainment with cloudy air for the value of $R' = 10^{-3}\ \text{sec}^{-1}$ (Fig. 4.4), while the liquid water content profile is situated between those resulting from entrainment with clear air and with cloudy air, in both cases assuming $R' = 10^{-3}\ \text{sec}^{-1}$, as shown in Fig. 4.6.

Effect of Entrainment on the Droplet Spectrum Evolution

To examine the magnitude of the effect of entrainment on the droplet spectrum evolution a comparison of the droplet spectra obtained by assuming entrainment with those obtained without entrainment is made.

Fig. 4.7A shows the evolution of the initial droplet spectrum given in Fig. 4.1, resulting from the adiabatic case (i.e. no mixing), plotted at $t = 0, 6, 9,$ and 11.5 min, in terms of the 'mass density distribution'. It indicates that a narrow 'condensation peak' appears quickly and then a 'coalescence tail' starts to form.

The irregularities appearing in the coalescence tail are due to numerical error produced by the fact that a quite narrow condensation peak is present towards the last few minutes.

The combination of condensation along with coalescence in the model is very important. This is due to the fact that the collection efficiency

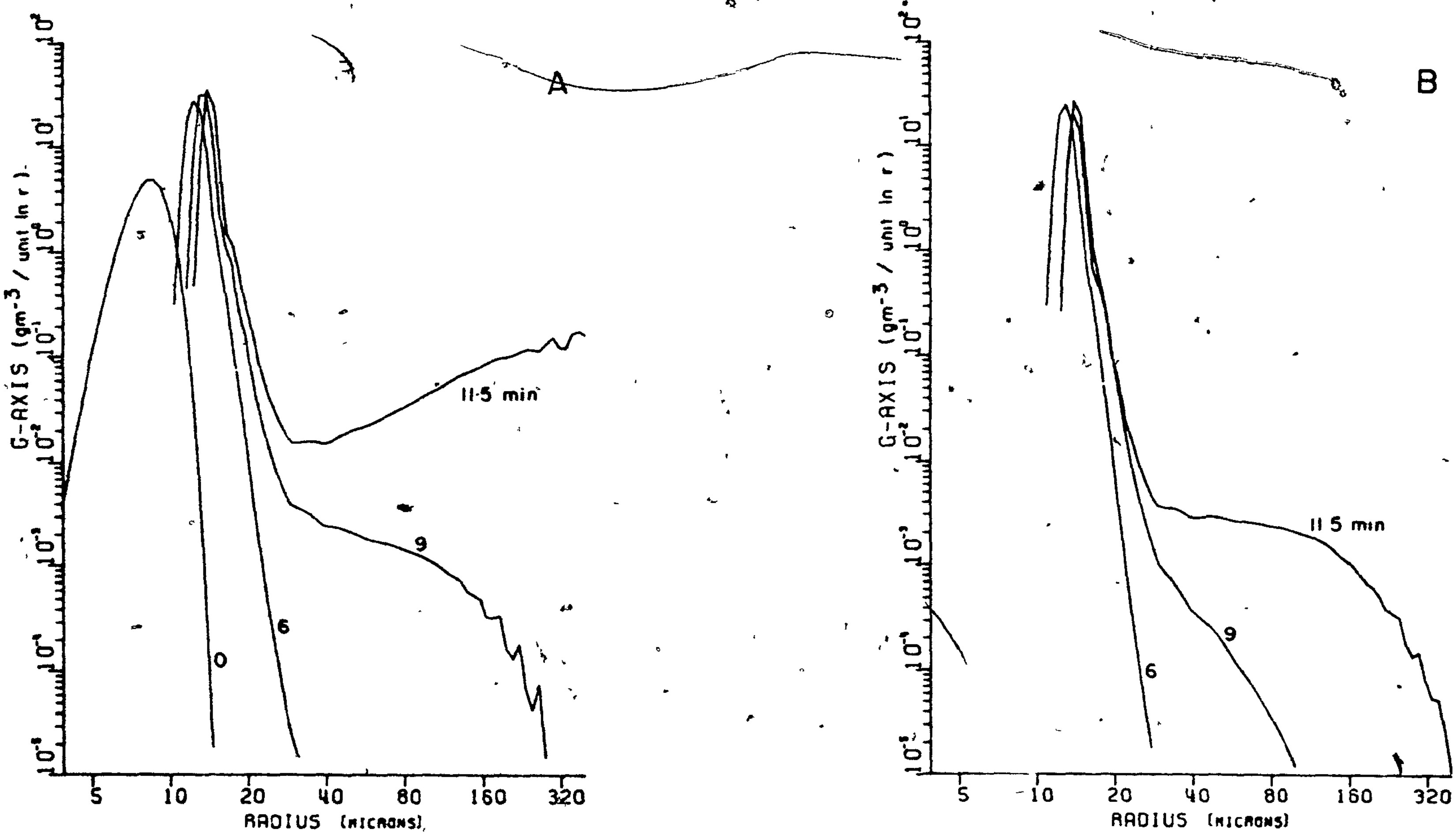

Fig. 4.7: Mass distribution, as a function of radius, for the continental case.

A: No entrainment, at time t = 0, 6, 9 and 11.5 min.

B: Entrainment with clear air, at time t = 6, 9 and 11.5 min, for $R' = 10^{-3}$ sec^{-1}.

is very low for small droplets but increases rapidly with the size of the droplets. Since condensation results in an increased mean radius the growth rate by coalescence increases significantly.

In other words the position of the condensation peak is important for further development of the distribution by coalescence. As the mean radius increases, more large droplets participate in the collection process and therefore the mass in the tail increases at a faster rate.

Thus the main features describing the development of the droplet spectrum are the 'condensation peak' due to growth by condensation, and the 'coalescence tail' due to growth by coalescence.

Now the effect of entrainment on these features will be described.

The resulting droplet spectra for the case of entrainment with clear air are shown in Figures 4.7B and 4.8A. They are plotted at $t = 6$, 9 and 11.5 min, for $R' = 10^{-3}\ \text{sec}^{-1}$ and $R' = 0.5 \times 10^{-3}\ \text{sec}^{-1}$ respectively. In addition, for comparison, the above droplet spectra are also plotted in Fig. 4.8B at the same time, i.e. 11.5 min, together with the one resulting from the adiabatic case.

This figure indicates that entrainment with clear air, for $R' = 10^{-3}\ \text{sec}^{-1}$, delays the development of the coalescence tail by approximately 2 minutes, with respect to that obtained in the adiabatic case. But by reducing the parameter R', to $R' = 0.5 \times 10^{-3}\ \text{sec}^{-1}$, this delay is reduced also by approximately the same factor.

Consequently the entrainment with clear air slows down the development of the coalescence tail and therefore the production of large droplets. Since the condensation peak in the case of entrainment with clear air is situated virtually at the same position as the one corresponding to the adiabatic case, the delay should be attributed to the fact that

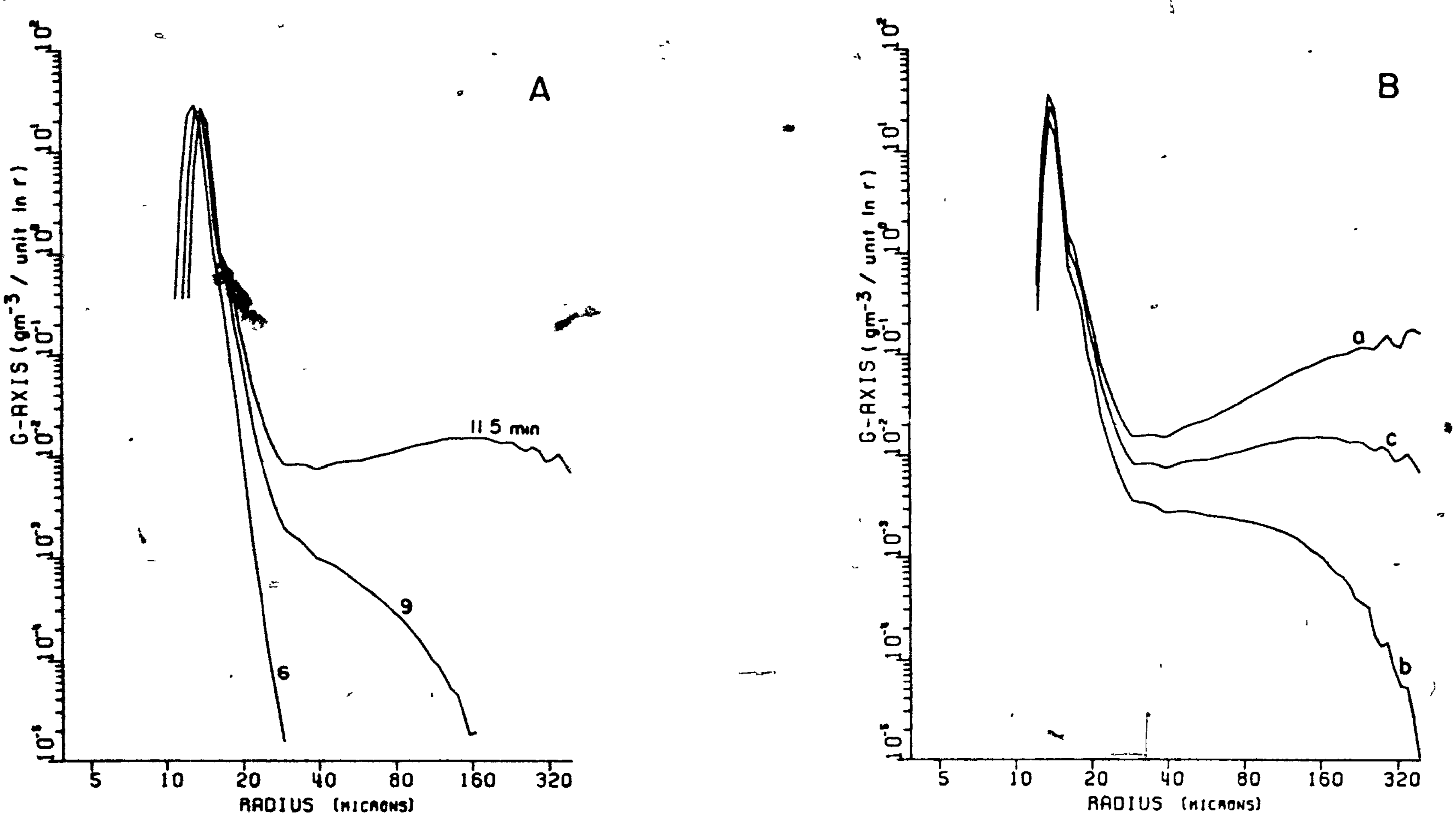

Fig. 4.8: Mass distribution, as a function radius, for the continental case.

A: Entrainment with clear, at time t = 6, 9 and 11.5 min, for $R' = 0.5 \times 10^{-3}$ sec^{-1}.

B: a) No entrainment at time t = 11.5 min b) and c) Entrainment with clear air, for values of $R' = 10^{-3}$ sec^{-1} and 0.5×10^{-3} sec^{-1} respectively, at time t = 11.5 min.

coalescence has not been as rapid because the number of droplets has been reduced.

Fig. 4.9 shows the variation of the droplet concentration with height (time) for the three cases: adiabatic case (i.e. no mixing), entrainment with clear air with $R' = 10^{-3}$ sec^{-1} and $R' = 0.5 \times 10^{-3}$ sec^{-1}. Equation (1) in the theory indicates that the rate of change of the number of droplets due to coalescence depends not only on the size of the droplets but also on their number. So the reduction of the droplet concentration due to entrainment with clear air delays the coalescence process, with respect to the adiabatic case. As the entrainment rate parameter increases the number of droplets decreases considerably and therefore coalescence becomes less rapid. On the other hand this dilution of the number of droplets prevents the condensation peak from shifting to the left relative to its position with no mixing, since its position is determined roughly by the ratio of the 'liquid water content' to the 'droplet concentration'. So in this case of entrainment with clear air the reduced liquid water content is distributed over a smaller number of droplets. That is why the position of the condensation peak is not influenced very much.

A measure of the development of the large droplets in the spectrum is provided by the radius of the 100th largest droplet per cubic meter, denoted by r_{100}. Therefore a plot of r_{100} as a function of height is given in Fig. 4.10 for the development of the distribution in the adiabatic case and with entrainment with clear air, for $R' = 10^{-3}$ sec^{-1} and $R' = 0.5 \times 10^{-3}$ sec^{-1}.

Similarly Fig. 4.11 shows the changes of the radar reflectivity factor Z with height, for the previously mentioned cases, which is also

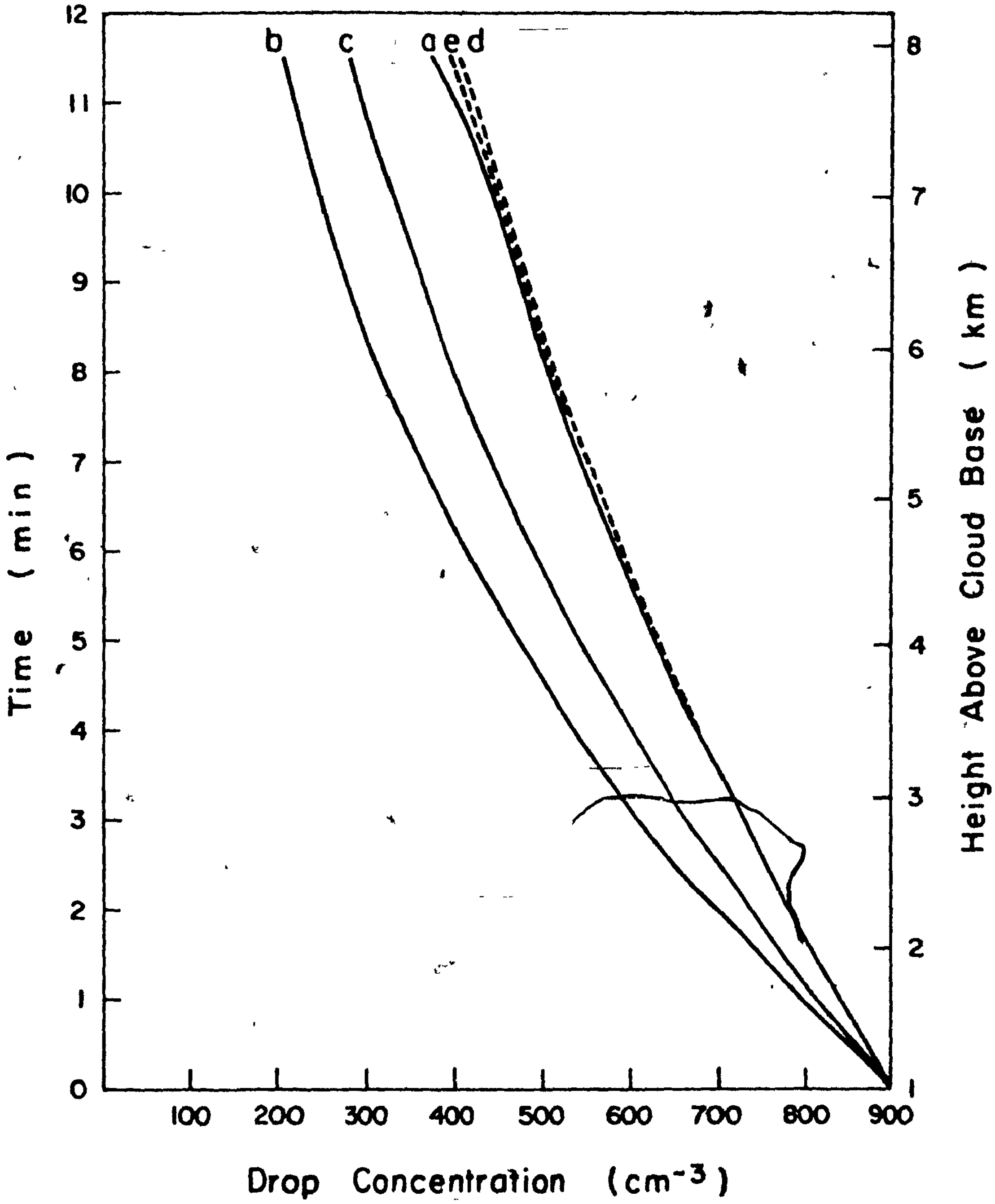

Fig. 4.9: Drop concentration, as a function of height, for the continental case.

a) No entrainment
b) and c) Entrainment with clear air, for $R' = 10^{-3}$ sec^{-1} and 0.5×10^{-3} sec^{-1} respectively.
d) and e) Entrainment with cloudy air, for $R' = 10^{-3}$ sec^{-1} and 0.5×10^{-3} sec^{-1} respectively.

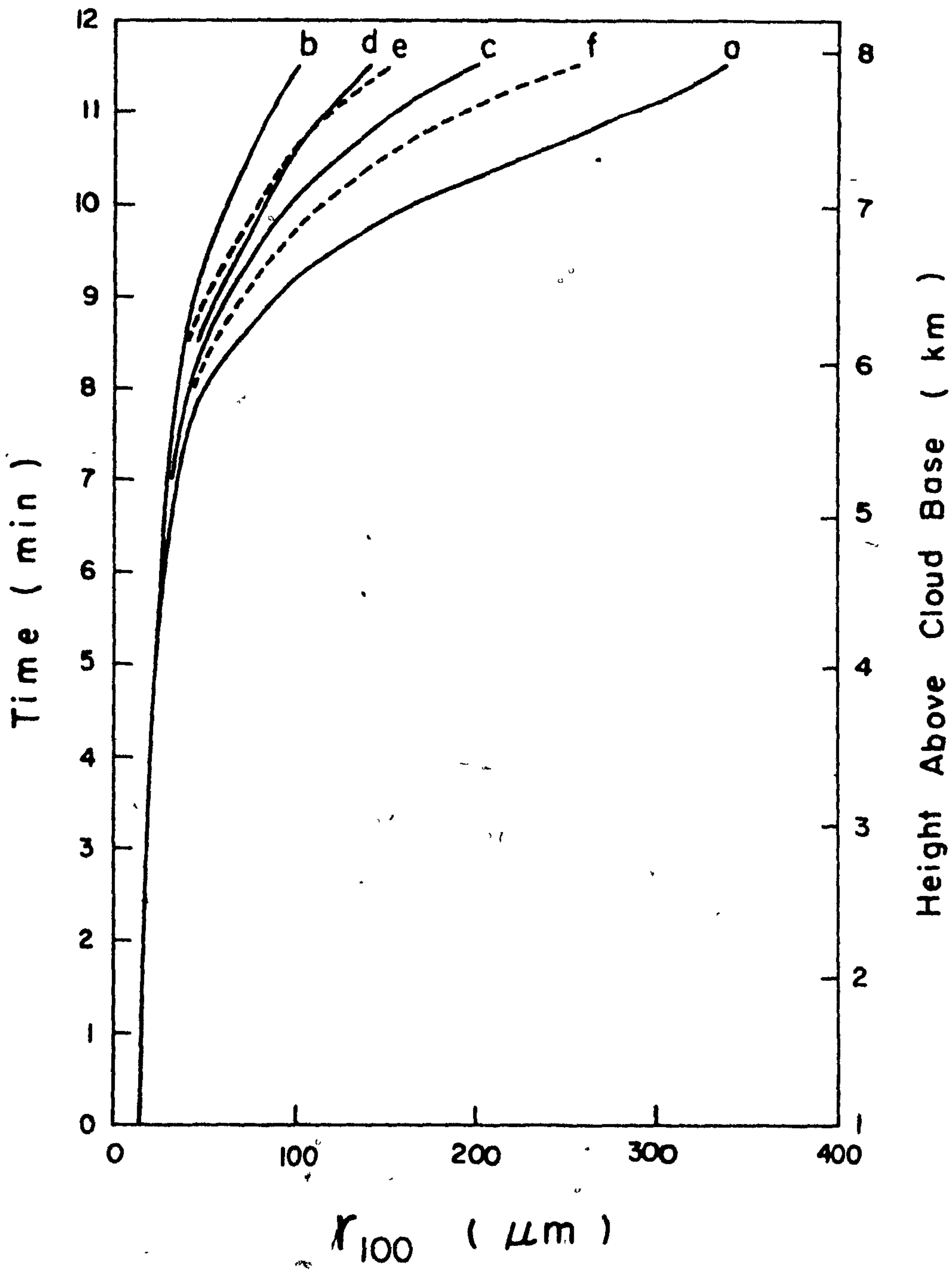

Fig. 4.10: The radius of the 100th largest drop m^{-3}, as a function of height, for the continental case.

(Solid lines) a) No entrainment b) and c) Entrainment with clear, for $R' = 10^{-3}$ sec^{-1} and 0.5×10^{-3} sec^{-1} respectively
d) Entrainment with clear saturated air, for $R' = 10^{-3}$ sec^{-1}

(Dashed lines) e) and f) Entrainment with cloudy air, for $R' = 10^{-3}$ sec^{-1} and 0.5×10^{-3} sec^{-1}, respectively.

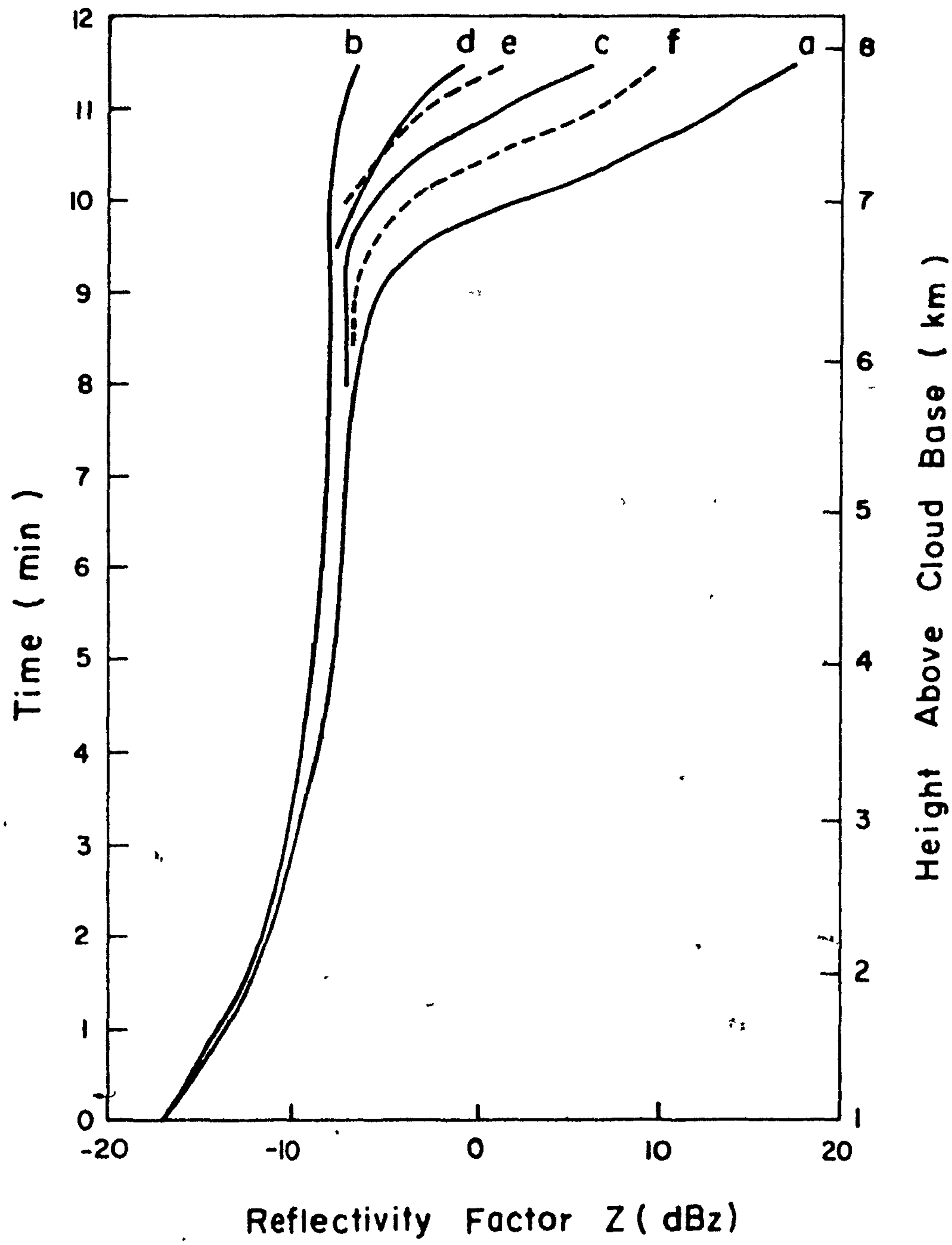

Fig. 4.11: The radar reflectivity factor Z, as a function of height, for the continental case.

(Solid lines) a) No entrainment

b) and c) Entrainment with clear air, for $R' = 10^{-3}$ sec^{-1} and 0.5×10^{-3} sec^{-1} respectively

d) Entrainment with clear saturated air, for $R' = 10^{-3}$ sec^{-1}

(Dashed lines) e) and f) Entrainment with cloudy air, for $R' = 10^{-3}$ sec^{-1} and 0.5×10^{-3} sec^{-1} respectively.

an indication of the development of the distribution.

In the adiabatic case r_{100} reached the value of 336 μm and the reflectivity factor the value of 17 dBZ at $t = 11.5$ min. When entrainment with clear air takes place, for $R' = 10^{-3}$ sec^{-1}, the corresponding values are 100 μm and -7 dBZ, while for $R' = 0.5 \times 10^{-3}$ sec^{-1} r_{100} reached the value of 200 μm and the reflectivity factor Z the value of 6 dBZ at the same time.

From the above we can conclude that entrainment with clear air does not reduce significantly the size of the drops that have grown by condensation but it is important because it slows down the production of large drops. In addition the results from both entrainment rate parameters indicate that by decreasing entrainment the production of large droplets becomes faster but always remaining slower than in the adiabatic case.

Now we will deal with the effect of entrainment with cloudy air (containing small droplets) on the droplet spectrum evolution for the same updraft conditions.

Figures 4.12 (A and B) show the evolution of the droplet spectra with time in this case. They are plotted at $t = 6$, 9, and 11.5 min, for $R' = 10^{-3}$ sec^{-1} and $R' = 0.5 \times 10^{-3}$ sec^{-1} respectively. In addition Fig. 4.13A shows the developed spectra at time $t = 11.5$ min, for entrainment with cloudy air at rates $R' = 10^{-3}$ sec^{-1} and 0.5×10^{-3} sec^{-1}, together with the adiabatic case at the same time. From the plots (not shown) of the spectra at different times it was found that development of the coalescence tail is delayed by approximately 100 sec, and 50 sec, for $R' = 10^{-3}$ sec^{-1} and 0.5×10^{-3} sec^{-1} respectively, relative to the adiabatic case.

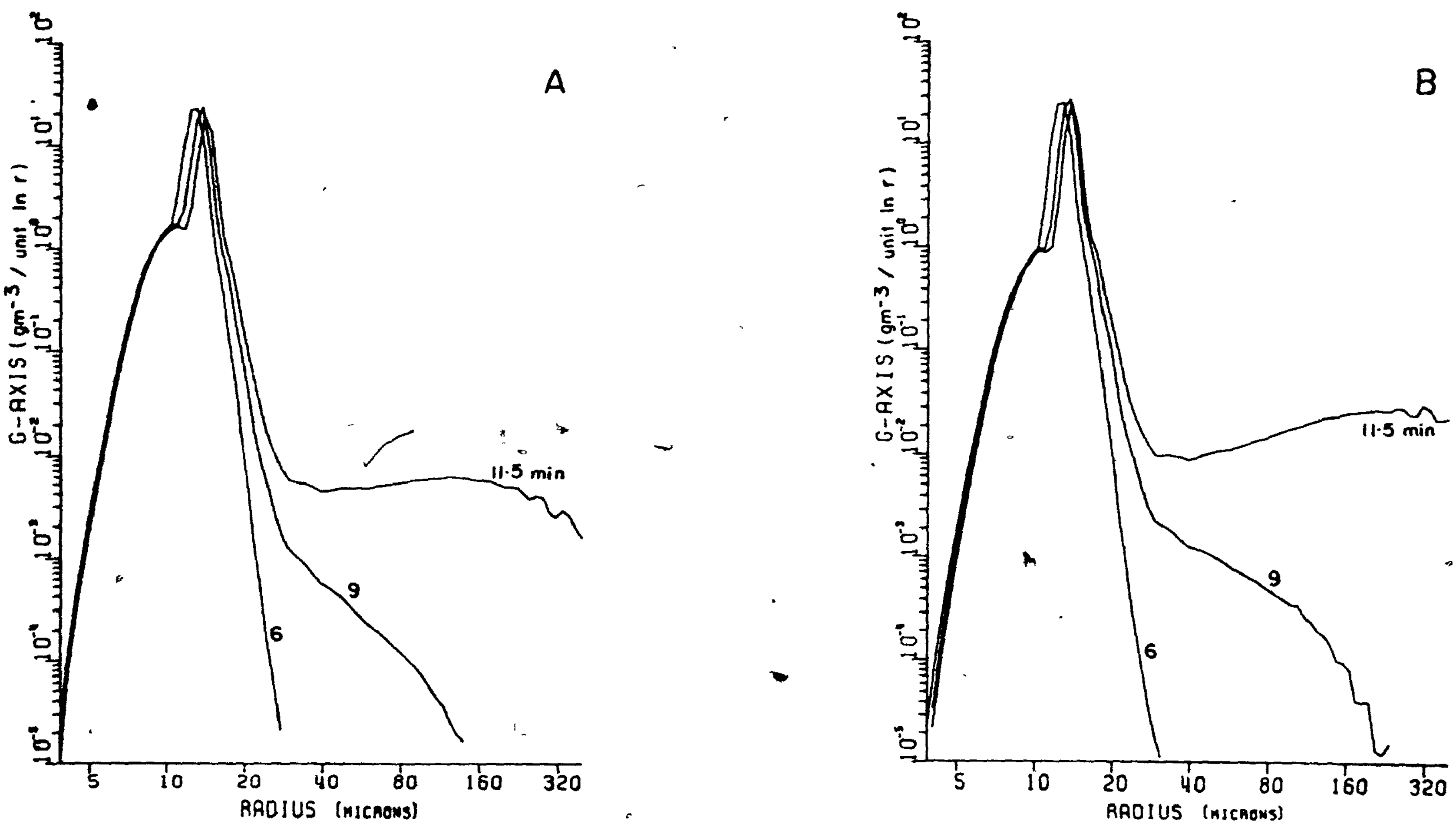

Fig. 4.12: Mass distribution, as a function of radius, for the continental cloud case, at time t = 6, 9 and 11.5 min.

A: Entrainment with cloudy air, for $R' = 10^{-3}\ sec^{-1}$

B: Entrainment with cloudy air, for $R' = 0.5 \times 10^{-3}\ sec^{-1}$.

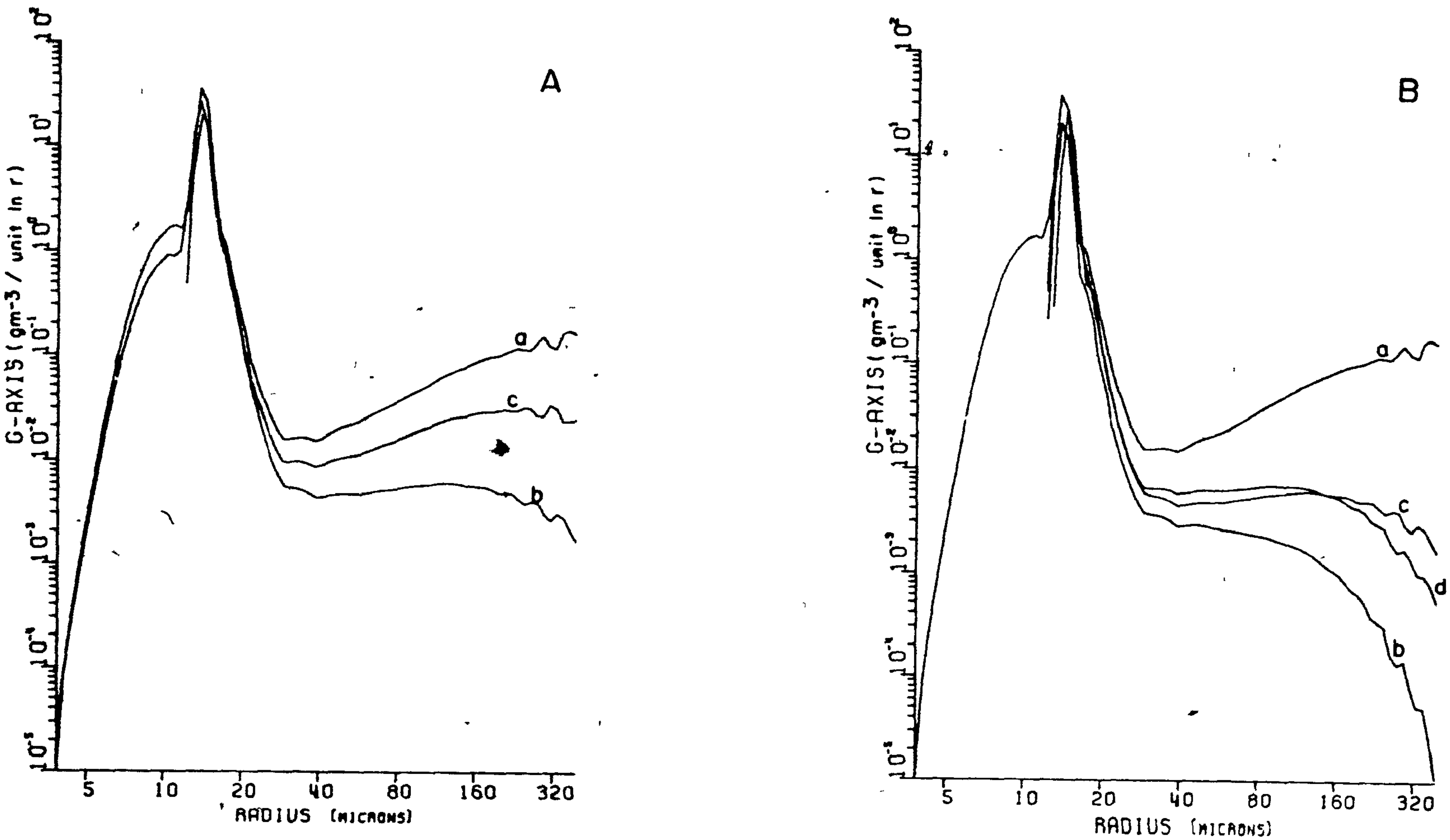

Fig. 4.13: Mass distribution, as a function of radius, for the continental case, at time t = 11.5 min.

A: a) No entrainment b) and c) Entrainment with cloudy air, for $R' = 10^{-3}$ sec^{-1} and 0.5×10^{-3} sec^{-1} respectively.

B: a) No entrainment b), c) and d) Entrainment with clear cloudy, and clear saturated air respectively, for $R' = 10^{-3}$ sec^{-1}.

A reason for this delay is that the number of droplets with radii corresponding to the condensation peak region or larger is reduced owing to entrainment. However Fig. 4.9, which shows the variation of the droplet concentration with height, indicates that in the case of entrainment with cloudy air the droplet concentration remains somewhat higher than in the adiabatic case after the first few minutes. This can be explained as follows. The droplet concentration of the developing droplet spectrum decreases because of two factors, namely the decrease of density with height and the collection process. On the other hand the entrained initial spectrum decreases its droplet concentration only because of the density decrease. Thus the concentration of the developing droplet spectrum is decreasing at a faster rate than the spectrum with entrainment. But the coalescence mechanism has only a slight effect on the droplet concentration in the first minutes, while it becomes more significant towards the end.

So the results indicate higher droplet concentration in particular towards the end. The entrained small droplets are accumulated mostly to the left side of the region of the condensation peak without involving the coalescence tail.

Also in this case, as in the case of entrainment with clear air, by doubling the entrainment rate parameter, the delay in the development of the coalescence tail is approximately doubled.

A comparison between the cases of entrainment with clear and cloudy air at the same rate is shown in Fig. 4.13B in which the droplet spectra are plotted for an entrainment rate $R' = 10^{-3}\ \sec^{-1}$ together with the adiabatic case, at $t = 11.5$ min. The figure indicates that in the case of entrainment with cloudy air the coalescence tail develops at a faster rate than in the case of entrainment with clear air. Taking into account that the entrained small droplets are accumulated at small radii, as mentioned before, the following explanation could be given. In the case of entrainment with cloudy air more condensation takes place than in the case of entrainment with clear air. This is why towards the end of the time period the condensation peak takes its final position, approximately at radius 14 μm, about 30 sec. earlier than in the case of entrainment with clear air. This could cause a faster development of the coalescence tail.

From the above we can conclude that entrainment with cloudy air slows down the production of large drops at a slower rate than entrainment with clear air.

This is shown also by Figures 4.10 and 4.11 in which the radius of the 100th largest droplet per cubic meter, (r_{100} - μm), and radar reflectivity factor, (Z-dBZ), are plotted as functions of height.

Finally we will discuss the results of entrainment of saturated air (not containing droplets), assuming one value of R' equal to 10^{-3} sec^{-1}.

Fig. 4.14 shows the developing spectrum at times t = 6, 9 and 11.5 min, in this case. For comparison in Fig. 4.13B the spectrum in the case of saturated (clear) air is also plotted at t = 11.5 min.

It is apparent that in this case, the rate of the development of the coalescence tail is very similar to that for entrainment with cloudy air.

On the other hand the condensation peak in the case of entrainment with saturated air is situated somewhat to the right of the position in which it is found in the case of entrainment with cloudy air and with unsaturated clear air for the same value of the parameter R'.

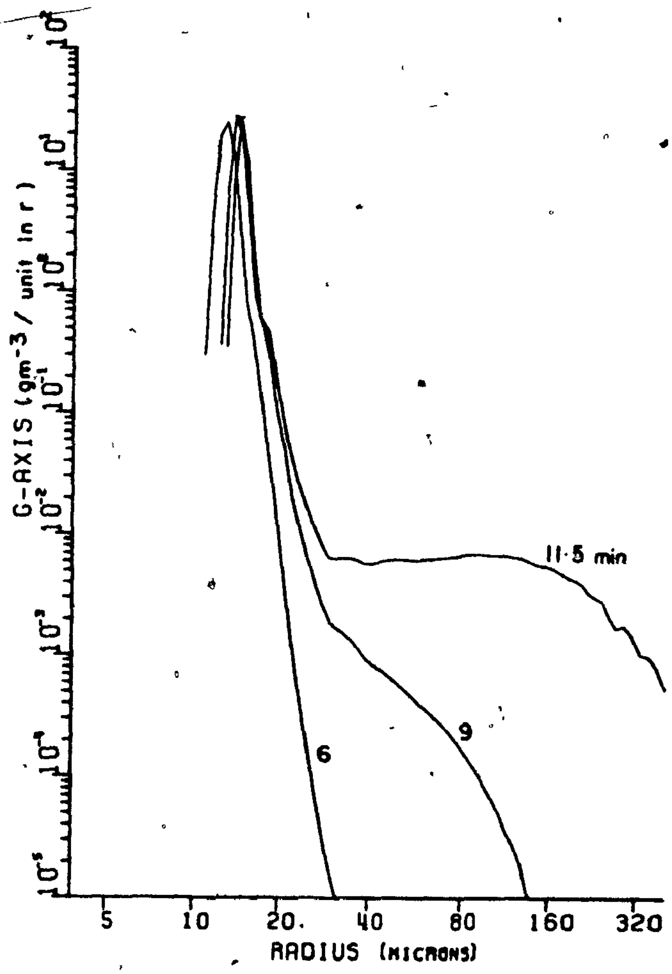

Fig. 4.14: Mass distribution, as a function of radius, for the continental case. Results of entrainment with clear saturated air, for $R' = 10^{-3}\ sec^{-1}$, at time $t = 6$, 9 and 11.5 min.

This can be explained by the fact that in the case of saturated air more condensation takes place than in the case of unsaturated (clear) air, while the total 'drop concentration' undergoes the same reduction. This is why the condensation peak is shifted somewhat to the right so the coalescence process becomes important earlier and therefore the development of the coalescence tail is faster than the clear air case.

While in the case of saturated clear air as well as in the case of cloudy air approximately the same condensation takes place, there is a difference in the total 'droplet concentration'. This is the reason why the condensation peak is situated approximately at radius $r = 15\ \mu m$, or specifically one interval of J to the right relative to the cloudy air case. It has taken this position at time $t = 10$ min.

The position of the condensation peak in the case of saturated clear air with respect to the cloudy air case would lead one to expect a more pronounced 'coalescence tail' in the former case compared to the latter. This does not happen, probably because in the case of cloudy air we get a broadened spectrum in the neighborhood of the 'condensation peak' while in the case of clear saturated air a narrower peak is present. Thus more droplets are able to participate in the collection process in the case of cloudy air. This might compensate for the development of the coalescence tail between the two cases. But in both cases the droplet spectra are developing essentially at the same rate.

So the entrainment with clear saturated air slows down the production of large drops approximately at the same rate as the entrainment with cloudy air relative to the adiabatic case. This is shown also by figures 4.10 and 4.11, in which the radius of the 100th largest droplet per cubic meter (r_{100}), and the reflectivity factor (Z), are plotted as functions of height (time).

4.3 Maritime cloud cases

In this section two cases are examined assuming conditions for Hawaii convective clouds.

Initial Distribution

The initial distribution is taken to be the same in both cases. Hawaiian clouds are characterized by relatively small numbers of cloud droplets (~100 cm^{-3}) having relatively large diameters (Rogers and Jiusto (1966)). Accordingly the following values of the parameters defining the initial distribution are taken:

N_o (cm^{-3})	$\bar{r}$ (μm)	ν
80	13	0

The initial value of liquid water content is then 0.74 gm^{-3}. Fig. 4.15 shows the resulting 'number distribution'. The dispersion in N(r) is approximately 0.5 ($\sigma_{\bar{r}} / \bar{r} \approx 0.5$).

Initial and Environmental Conditions

CASE I

In 1954 aircraft observations over the sea upwind of the Island of Hawaii were made (Johnson (1957)).

During this project detailed vertical soundings of temperature and water vapor content for nine non-consecutive days were taken. The data of one of these days, 21st of October 1954, are used as environmental conditions for this case. Also the position of the average cloud base on

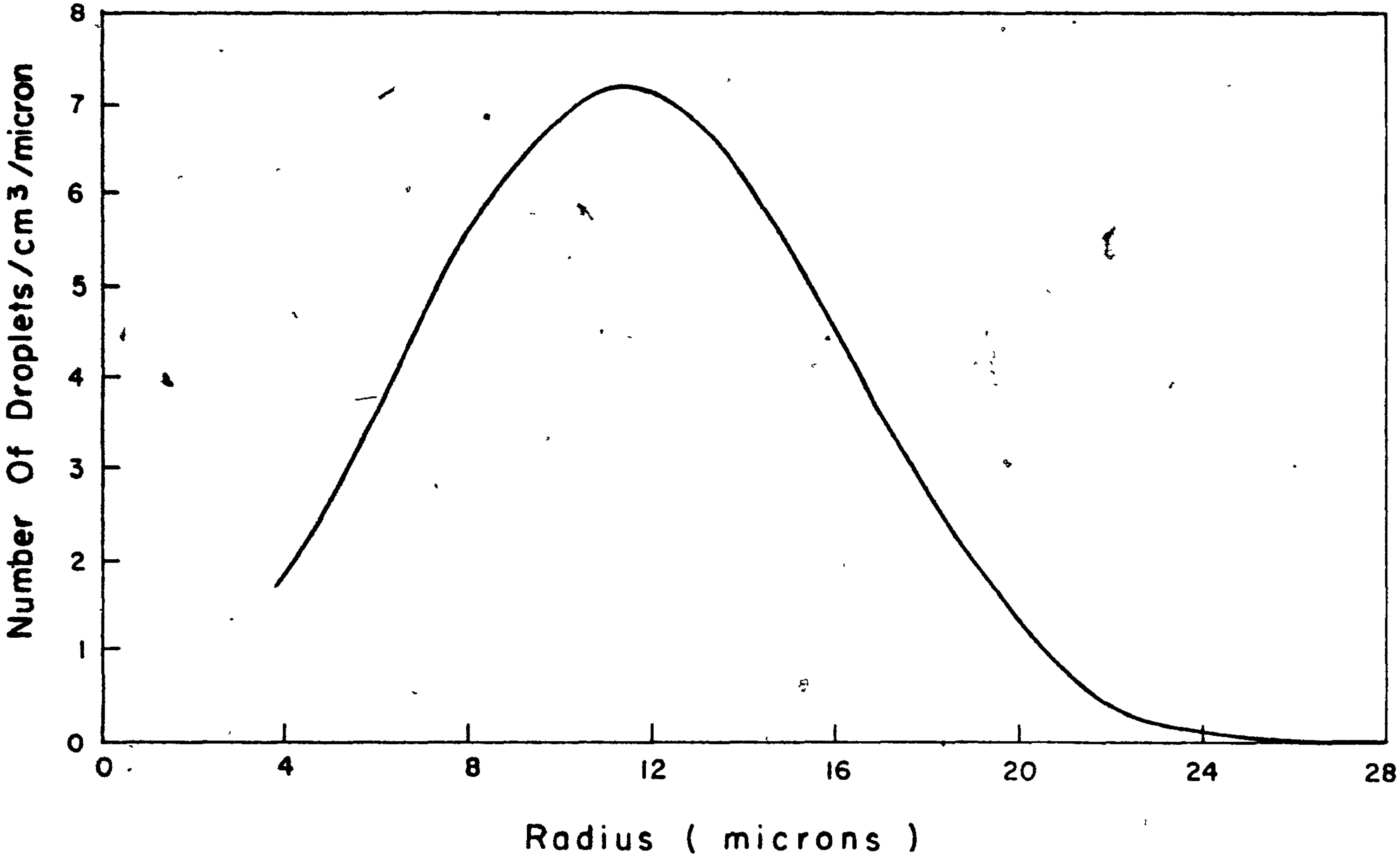

Fig. 4.15: Initial distribution for the maritime cases. (N_o = 80 cm^{-3})

this day is given. The weather on 21 October is described as follows.

"A few light showers were observed off the coast during the flight, while the orographic cloud was well developed and substantial rain fell on the mountain slopes" (Johnson (1957)).

From the measurements the cloud base is taken at 700 m at 18°C temperature. Its position is very near to the lifting condensation level (LCL). Fig. 4.16A shows the environmental conditions and the adiabatic parcel temperature. A characteristic of this environment is that the relative humidity is about 80% up to the inversion layer.

The updraft velocity is assumed constant with height at a value of 2.5 m/sec. This value is reasonable for Hawaii convective clouds as shown by computed values of updraft velocity for some days with convective activity in Hawaii (Rogers (1967)).

With the above conditions the effect of entrainment with clear air and with cloudy air is calculated assuming for the entrainment rate parameter the value of $R' = 10^{-3}\ sec^{-1}$.

The calculations started 300 m above cloud base where the adiabatic liquid water content is equal to the water contained in the initial droplet spectrum, namely 0.74 gm^{-3}, and was terminated at a height of 2350 m, approximately where the inversion layer is found.

CASE II

The main difference of this case from the first one is in the choice of the environmental parameters.

These conditions do not refer to a particular day but are mean conditions for the period 11 July to 25 August 1965 for Hilo. (Lavoie (1967)).

Accordingly the environmental conditions are taken from the "Mean

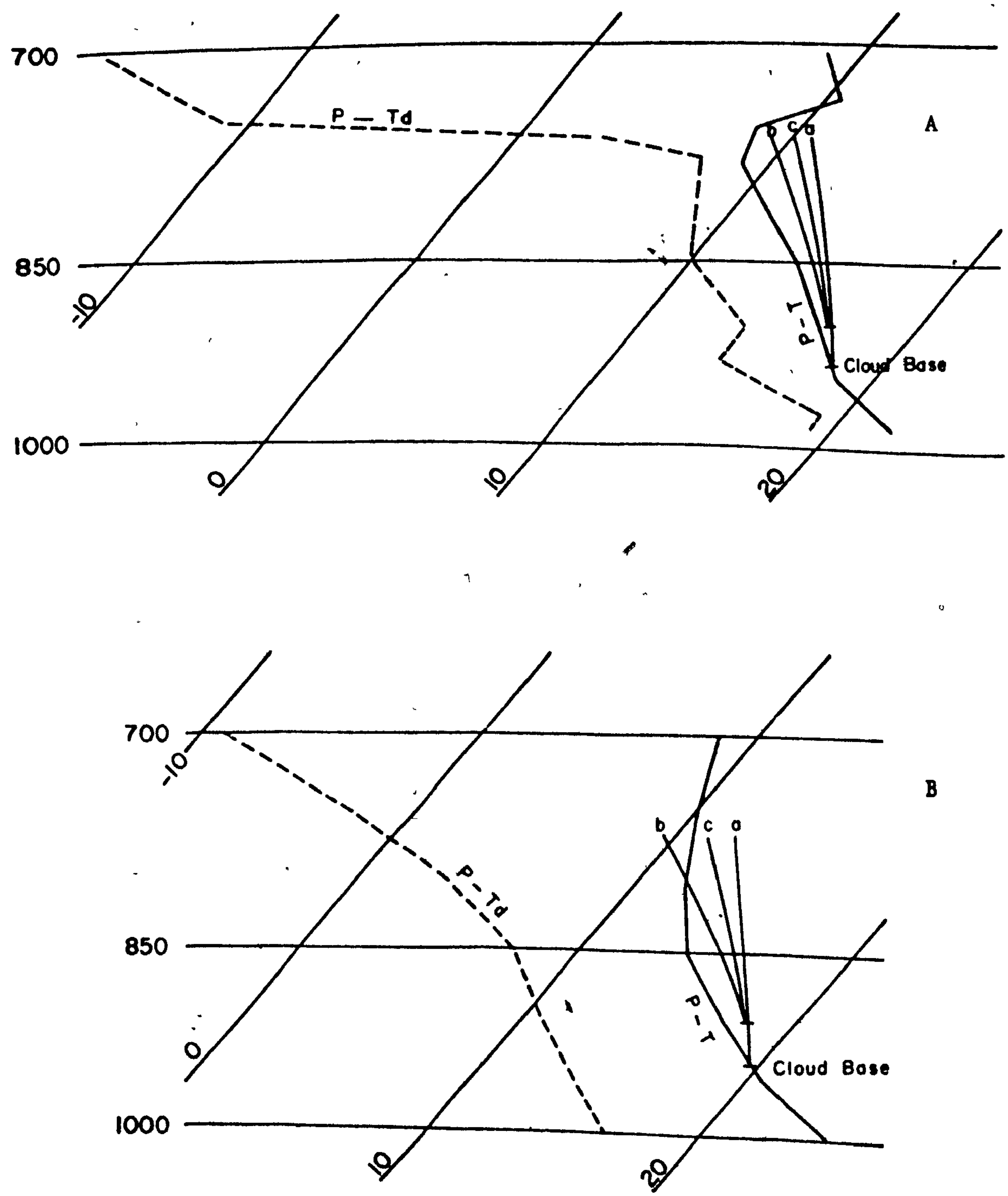

Fig. 4.16: Figures A and B represent the initial and environmental conditions, for the maritime cases (I) and (II), respectively. In both figures the temperature profiles are: a) No entrainment b) and c) Entrainment with clear and cloudy air respectively, for $R' = 10^{-3}$ sec^{-1}.

Hilo Radiosonde Data' for temperature and mixing ratio at different pressure levels at time (00 GMT). The cloud base is taken at 670 m (MSL), height which is given as the median value for this period at the same time. The cloud base temperature is taken to be 19.5°C to coincide with the temperature of the environment at this height. These cloud base conditions are not consistent with the LCL or mixing condensation level (MCL), due to the way they were chosen. This inconsistency would have little effect on the entrainment calculations, the purpose of which is to see the magnitude of the influence of the entrainment of an environment of lower relative humidity, since the relative humidity of this environment is approximately 60% up to the inversion layer while in the previous case it was about 80%. Fig. 4.16B shows the environmental conditions and the adiabatic parcel temperature.

The calculations carried out started with the same initial distribution and assuming the same value of vertical velocity as the previous maritime case. Also the initial height is 290 m above the cloud base. The total elapsed time is 9 min.

With the above conditions the development of the droplet distribution is calculated with clear and cloudy air for the same value of the entrainment rate parameter R', namely 10^{-3} sec^{-1}.

4.4 Results from the Maritime cases

Figures 4.16A and 4.16B, show the deviations of the calculated temperatures from those predicted by parcel theory, as a function of height when entrainment takes place with clear air and with cloudy air for the value of $R' = 10^{-3}$ sec^{-1}, for both maritime cases respectively.

Figures 4.17 and 4.18, show the deviations of the liquid water content from the adiabatic values, as a function of height when entrainment takes place also with clear and cloudy air for the same value of R', for both maritime cases.

From these figures, which show the changes of the thermodynamic properties of the cloud parcel due to entrainment it becomes clear that again entrainment reduces the temperature and the liquid water content of the cloud relative to the adiabatic values. Also entrainment with cloudy air reduces these properties at a slower rate than the entrainment with clear air. Of these two maritime cases the smaller decrease of both properties occurs in the case in which the clear air environment has higher relative humidity, as was expected.

Now we will deal with the developing droplet spectra. Fig. 4.19 is a plot of the droplet spectra for the adiabatic case (I), at time t = 0, 3, 6, and 9 min. Fig. 4.20A is a plot of the droplet spectra at time t = 9 min for the adiabatic case (no mixing) and for the case of entrainment with clear and cloudy air, for the first case in which the relative humidity of the environment is about 80%.

Thus we see that entrainment with clear and cloudy air both affect the droplet spectrum development of maritime clouds in a similar way to continental clouds. In other words entrainment slows down the development of the droplet spectrum and therefore the production of large drops. However, this influence seems to be not as destructive in the maritime clouds as it is for continental clouds. This becomes clear in Fig. 4.21 which shows the changes of the radius of the 100th largest droplet per cubic meter (r_{100}) and the radar reflectivity factor (Z) as a function of height, for the present case. It is indicated that when entrainment with

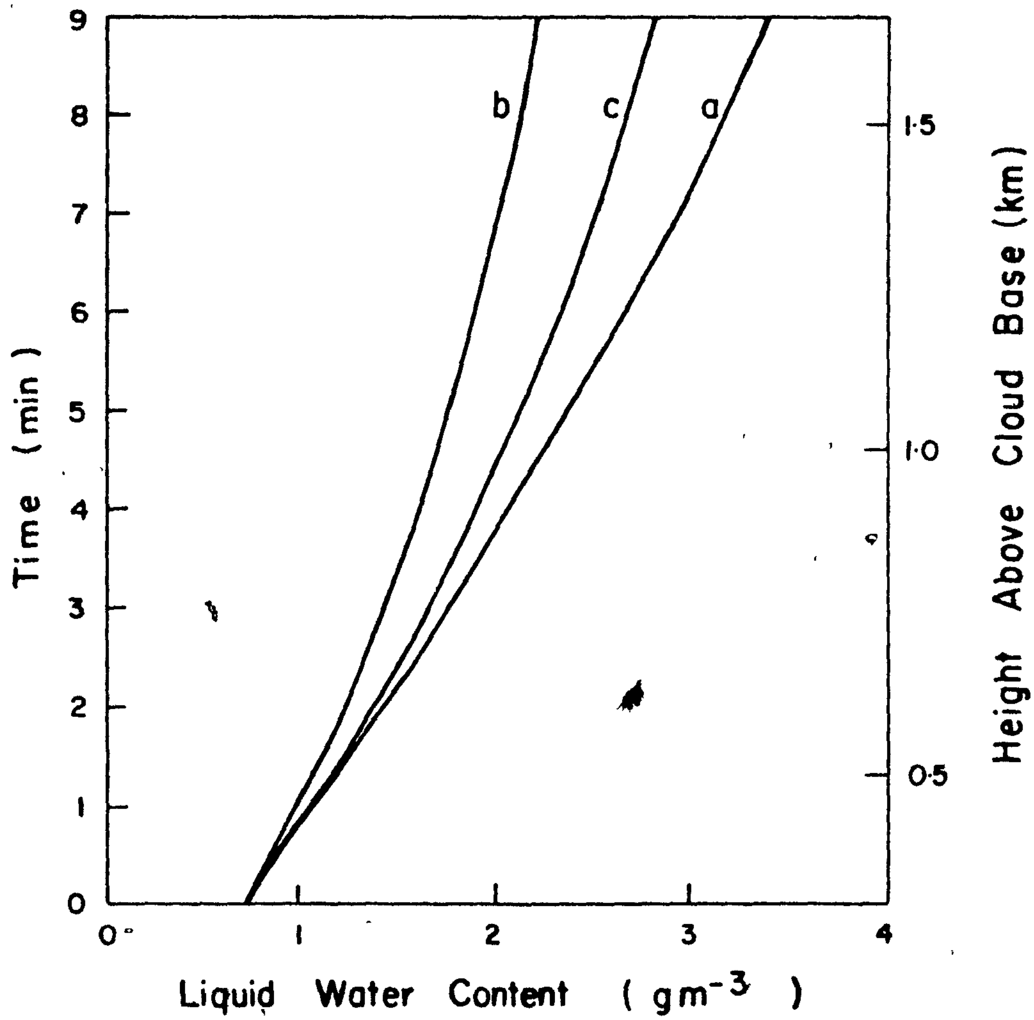

Fig. 4.17: Liquid water content profiles, as a function of height, for the maritime case (I).

a) No entrainment
b) and c) Entrainment with clear and cloudy air respectively, for $R' = 10^{-3}\ sec^{-1}$.

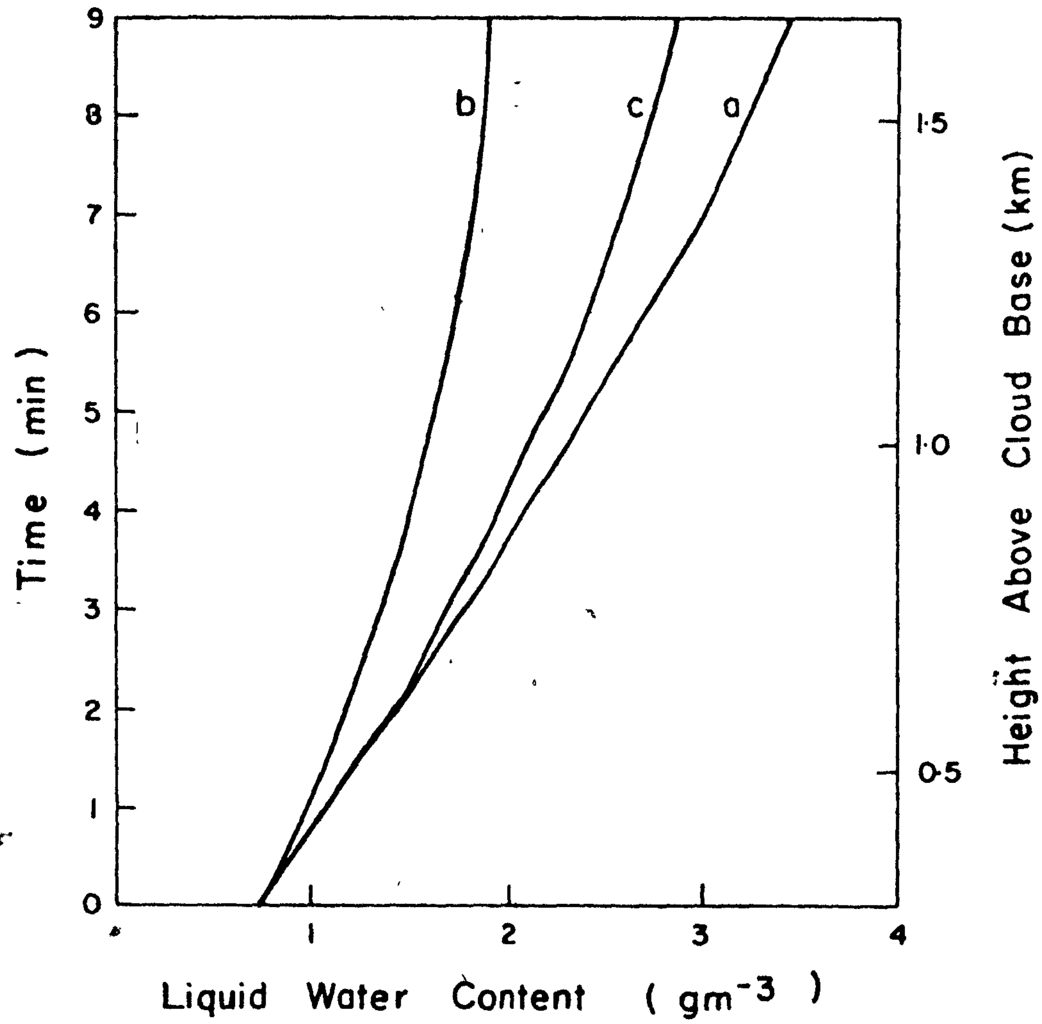

Fig. 4.18: Liquid water content profiles, as a function of height, for the maritime case (II).

a) No entrainment
b) and c) Entrainment with clear and cloudy air respectively, for $R' = 10^{-3}\ sec^{-1}$.

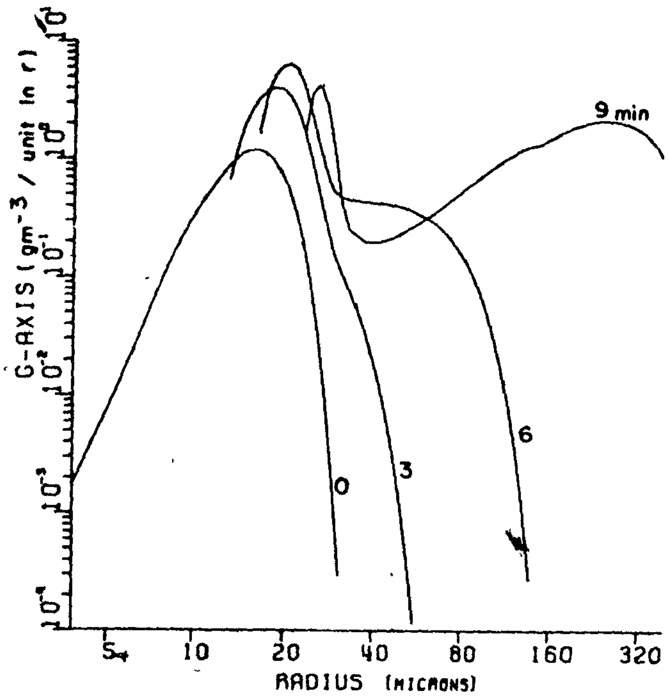

Fig. 4.19: Mass distribution, as a function of radius, for the maritime case (I), when no entrainment takes place after 0, 3, 6 and 9 min.

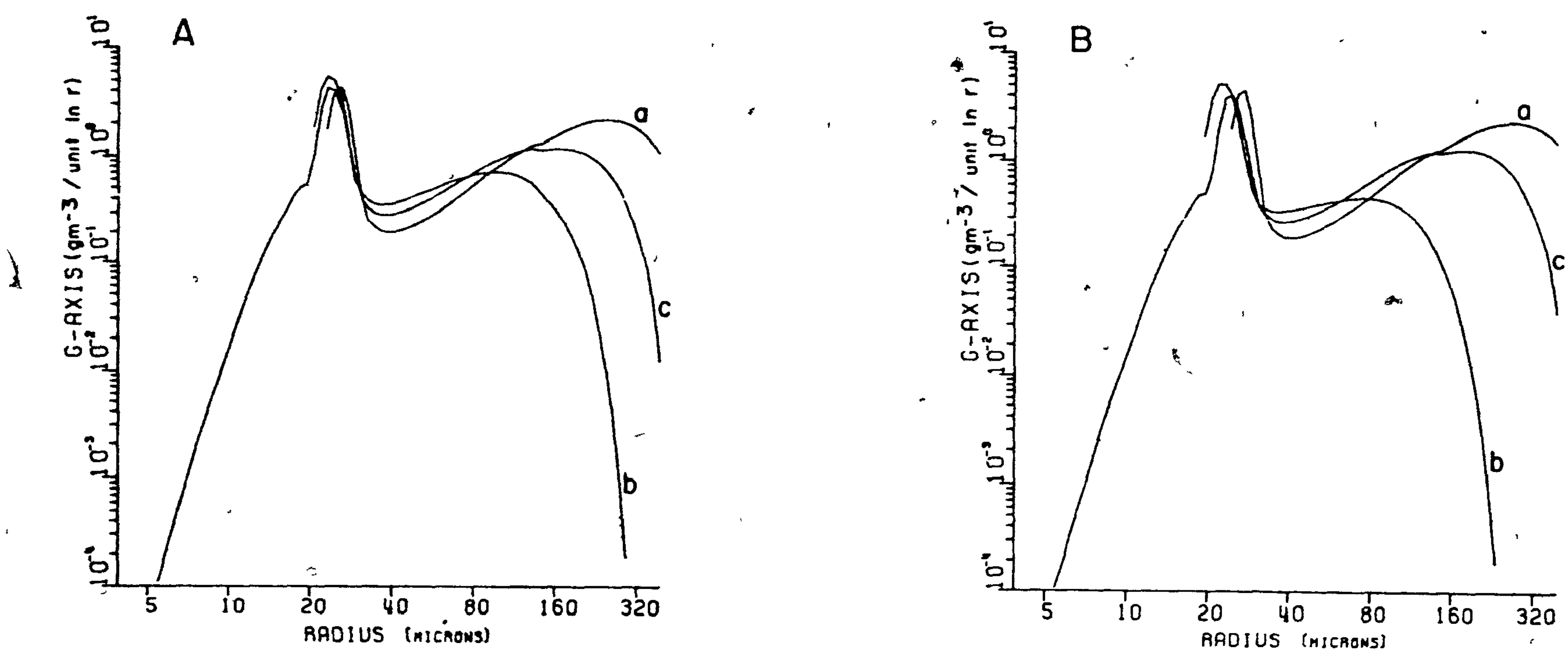

Fig. 4.20: Mass distribution, as a function of radius, for the maritime cases I (A) and II (B), at time t = 9 min. In both figures: a) No entrainment b) Entrainment with clear air, for $R' = 10^{-3}\ sec^{-1}$ c) Entrainment with cloudy air, for $R' = 10^{-3}\ sec^{-1}$.

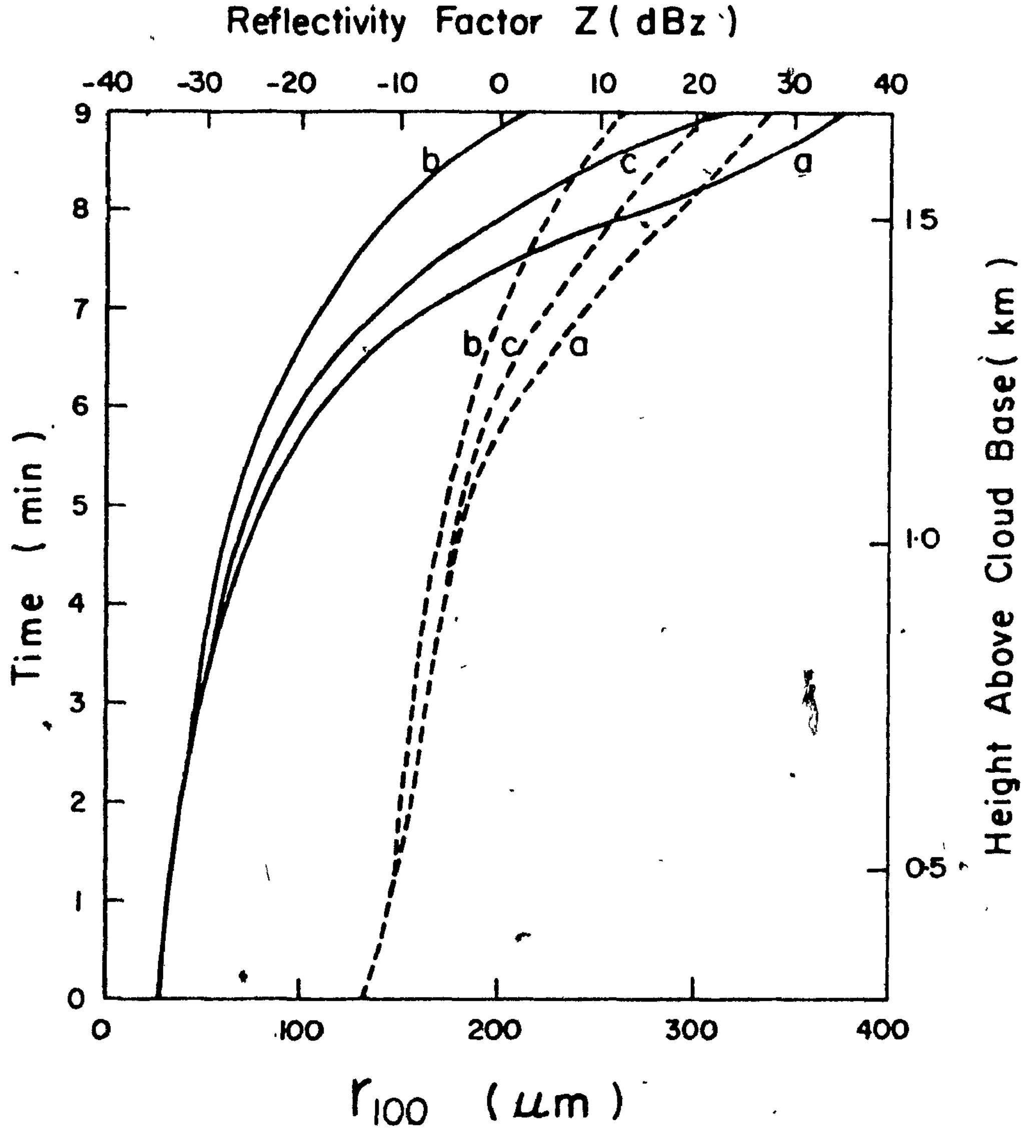

Fig. 4.21: The radar reflectivity factor (dashed lines), and the radius of the 100th largest drop m^{-3} (solid lines) for the maritime case (I). In both cases the curves are:

a) No entrainment
b) and c) Entrainment with clear and cloudy air respectively, for $R' = 10^{-3}\ sec^{-1}$.

clear air takes place, r_{100} takes the value of 212 μm while Z reached the value of 12.6 (dBZ) at time t = 9 min.

Fig. 4.22, shows the change of the droplet concentration as a function of height, in the adiabatic case and when entrainment with clear and cloudy air takes place for $R' = 10^{-3}$ sec^{-1} . We see that at the very last steps (~9 min) in the adiabatic case (no mixing) the drop concentration is approximately one half of that found when entrainment with clear air takes place. This is due mainly to the collection process. Since the size of the droplets becomes bigger in particular towards the end of the time, the collection process becomes important. During the last minute of the calculations the drop concentration in the boundary (radius 400 μm) starts to increase, which leads to a loss of drops at the end of the spectrum. However, this effect is negligible compared to the total drop concentration, for the time interval considered.

The big reduction of the drop concentration in the adiabatic case prevents the condensation peaks in the adiabatic case and in the case with entrainment from being situated in the same position, as they were in the continental case.

Finally Fig. 4.20B shows the developing droplet spectra for the second maritime case examined, namely the one with a lower relative humidity environment, at time t = 9 min, with and without entrainment.

A slight difference in the development of the droplet spectrum when entrainment with clear air takes place is indicated. Although the coalescence tail is developed similarly in both maritime cases, when no entrainment takes place, in the case of entrainment with clear air (60% relative humidity) there is a slightly slower development, as was expected. All the other properties, such as r_{100}, Z and N, plotted as functions of

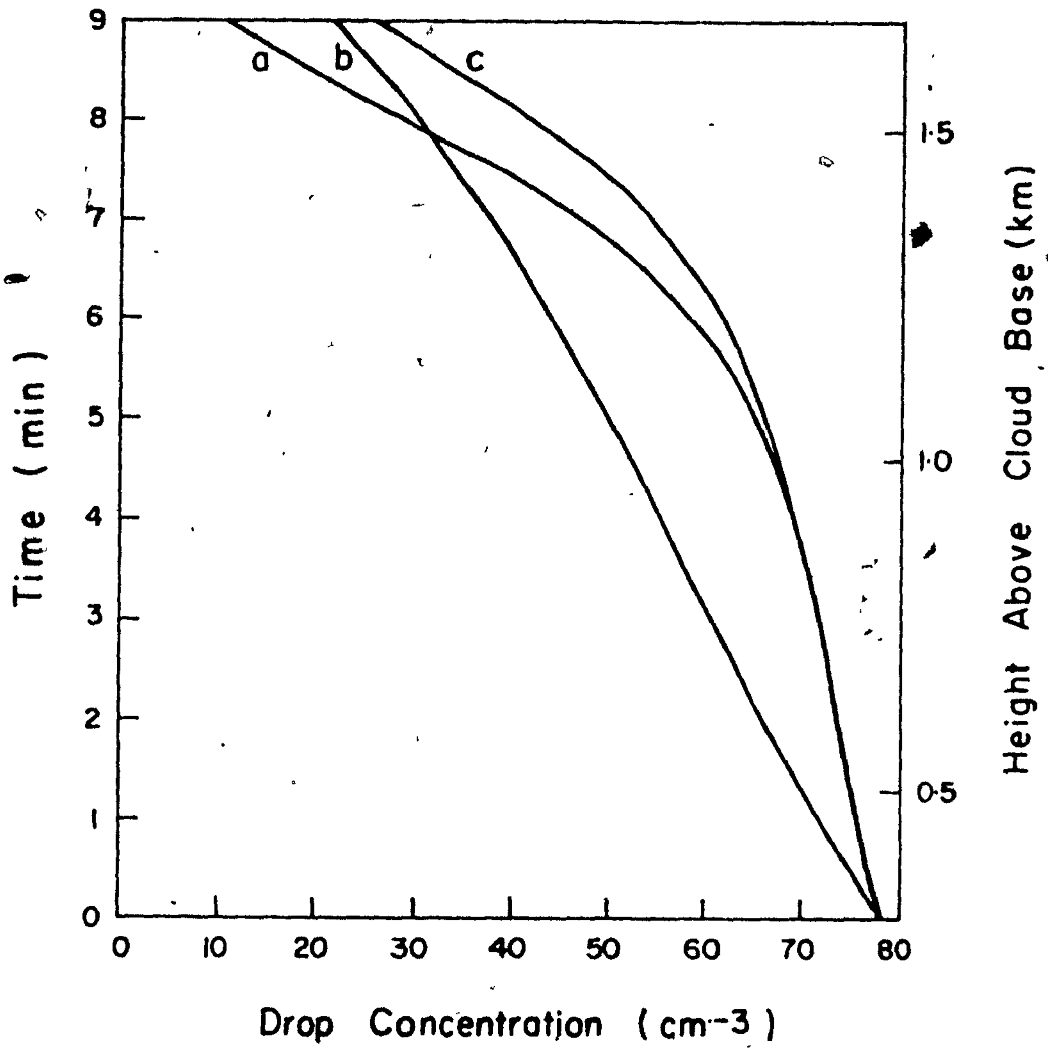

Fig. 4.22: Drop concentration, as a function of height, for the maritime case (I).

a) No entrainment
b) and c) Entrainment with clear and cloudy air respectively, for $R = 10^{-3}\ sec^{-1}$.

height in Figures 4.23 and 4.24 respectively, behave in similar ways.

From both maritime cases examined it is indicated that entrainment with clear air, for the value of the parameter R' equal to 10^{-3} sec^{-1}, delays the development of the droplet spectrum by approximately 2 min, while entrainment with cloudy air delays its development by approximately 1 min, for the same value of R'.

4.5 Simulation of entrainment in the adiabatic case

Now an attempt is made to see what the effect is of reducing artificially the adiabatic values of the liquid water content and simultaneously the drop concentration by an appropriate factor, while the temperature and the other parameters of the ascending cloud parcel remained unaltered. The reducing factor was chosen from the results as will be seen later.

This approach is useful from the point of view that in a more complicated model it might well be convenient if the clear air entrainment effect could be approximated by just reducing the drop concentration and the liquid water content. Also the cloudy air entrainment effect can perhaps be approximated by reducing only the liquid water content, since the drop concentration is approximately the same as for the adiabatic case.

To accomplish this, two experiments were attempted, one to compare the clear air entrainment effect and a second corresponding to the cloudy air entrainment effect, in the continental cloud case.

The previous results give the ratio of the liquid water content when entrainment with clear and cloudy air takes place, to the adiabatic liquid water content of the parcel when calculations were terminated. So for the continental case this ratio, at time t = 11.5 min, was 0.55 for

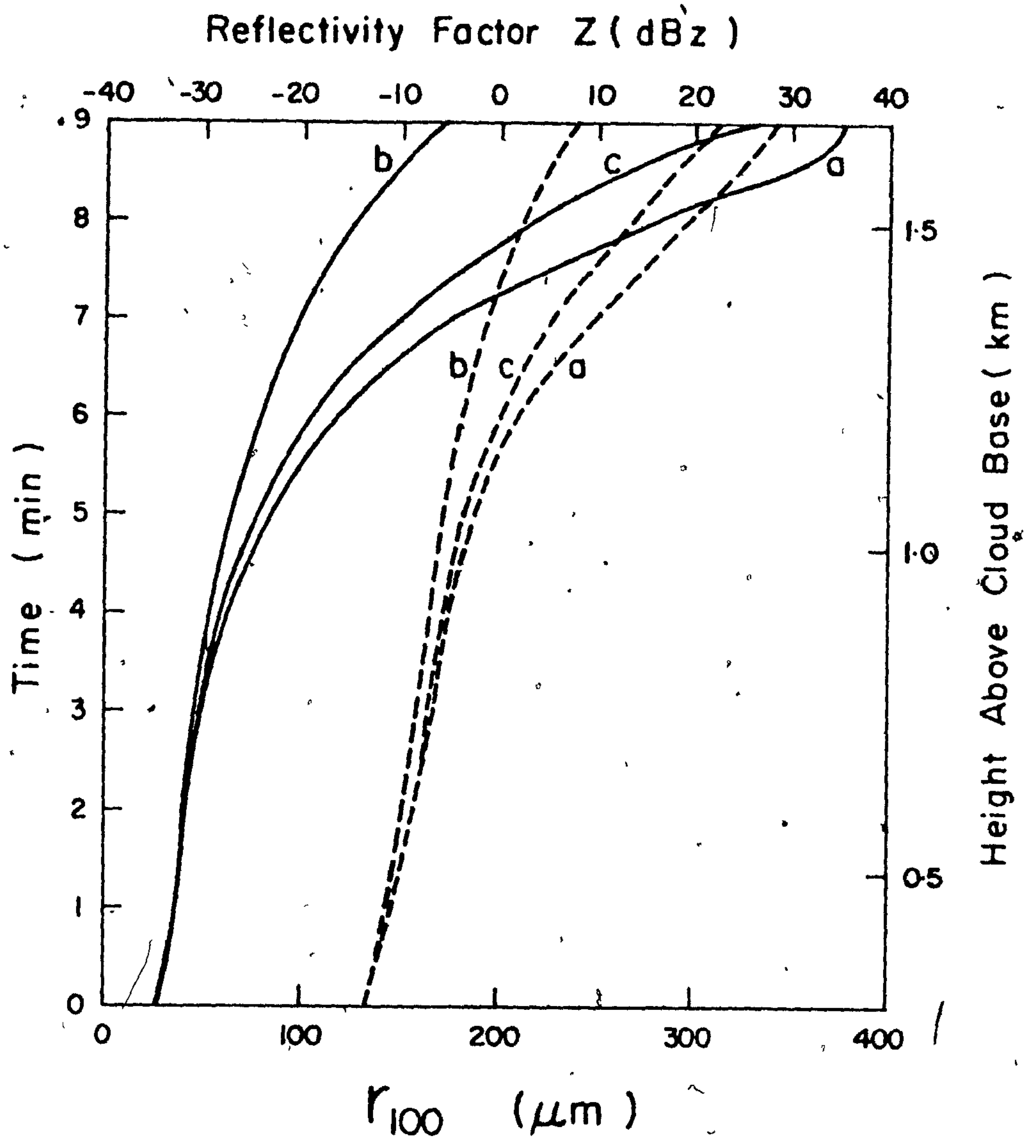

Fig. 4.23: The radar reflectivity factor (dashed lines), and the radius of the 100th largest drop m^{-3} (solid lines), for the maritime case (II) .

In both cases the curves are:
a) No entrainment
b) and c) Entrainment with clear and cloudy air respectively, for $R' = 10^{-3}$ sec^{-1}.

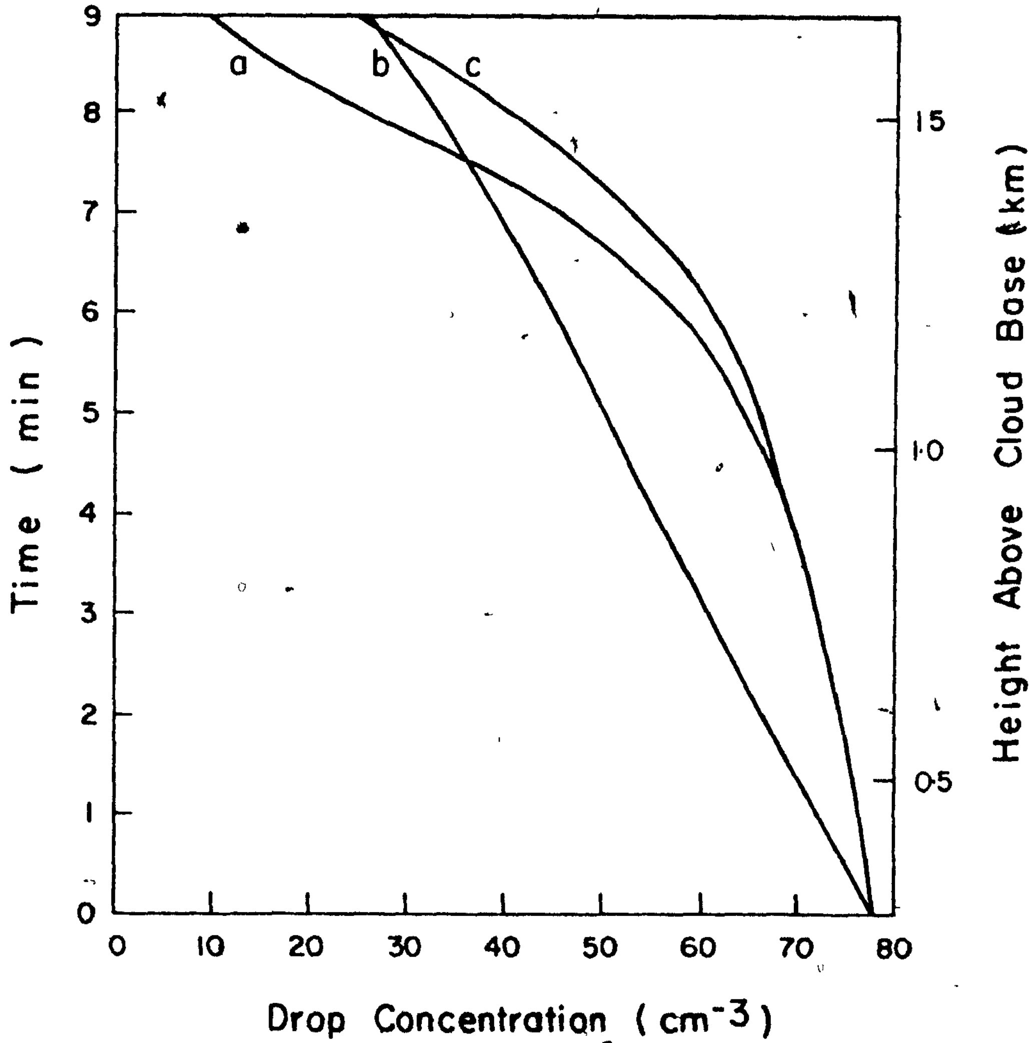

Fig. 4.24: Drop concentration, as a function of height, for the maritime case (II).

a) No entrainment
b) and c) Entrainment with clear and cloudy air respectively, for $R' = 10^{-3}$ sec^{-1}.

the clear air case and 0.74 for the cloudy air case, assuming $R' = 10^{-3}\ sec^{-1}$. In the maritime cases this ratio varies according to the relative humidity of the environment. Thus for the 60% relative humidity environment the values for clear and cloudy air were 0.55 and 0.83 respectively, while for the 80% relative humidity environment the values were 0.65 and 0.82 corresponding to clear and cloudy air cases, at time $t = 9$ min.

Thus, we tried to simulate the clear air entrainment effect, in the continental case for $R' = 10^{-3}\ sec^{-1}$, by the following two simultaneous procedures: first by applying a reducing factor of 0.6 to the adiabatic values of liquid water content, and second by reducing the drop concentration at each time step by the factor of 10^{-3}. It should be noticed that for the case of entrainment with clear air, for $R' = 10^{-3}\ sec^{-1}$ and for continental cloud conditions, it was found that at time $t = 11.5$ min the ratio of the drop concentration with entrainment to that without entrainment is also 0.55. Fig. 4.25A is a plot of the resulting spectrum at time $t = 11.5$ min together with that resulting from entrainment with clear air and the adiabatic case at the same time. It indicates that the factor 0.6 gives a development of the coalescence tail at a somewhat lower rate than the calculation with entrainment of clear air. On the other hand, the position of the condensation peak is somewhat to the right due to the fact that proceeding in this way over the first portion of the ascent we get less condensation and over the last portion we get more condensation than with the entrainment calculation. But this is an indication that we can simulate approximately the clear air entrainment calculations, in this simple way.

As far as the cloudy air is concerned two values of the reduction

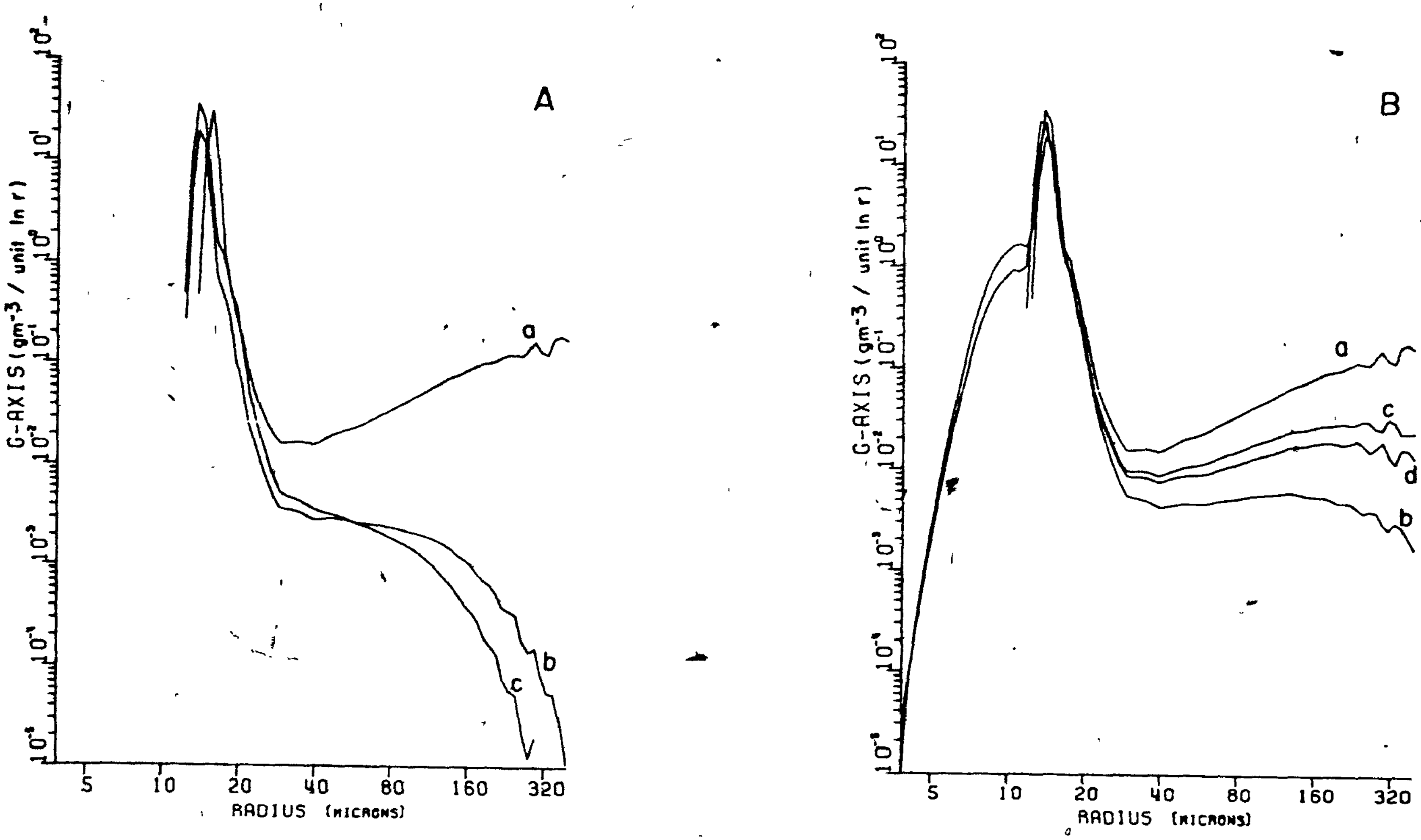

Fig. 4.25: Mass distributions at time t = 11.5 min, for the continental case.

A: a) No entrainment b) Entrainment with clear air, for $R' = 10^{-3}$ sec^{-1} c) The resulting spectrum where factor of 0.6 was applied to the adiabatic values of water content while the drop concentration was reduced by 10^{-3} sec^{-1}.

B: a) No entrainment b) and c) Entrainment with cloudy air, for $R' = 10^{-3}$ sec^{-1} and 0.5×10^{-3} sec^{-1} respectively d) The resulting spectrum when factor of 0.9 was applied only to the adiabatic values of water content.

factor were tested.

First the factor 0.74 given from the results, resulting in a spectrum (not shown), after 11.5 min, which was not in a reasonable agreement with the cloudy air case ($R' = 10^{-3}\ sec^{-1}$.)

Then the factor of 0.9 was tested resulting in the spectrum given in Fig. 4.25B together with the cloudy air case for $R' = 10^{-3}\ sec^{-1}$ and $0.5 \times 10^{-3}\ sec^{-1}$, and the adiabatic case after 11.5 min.

It is apparent that the coalescence tail is situated between the two cloudy air case spectra, and nearer to the cloudy case with $R' = 0.5 \times 10^{-3}\ sec^{-1}$. It must be noticed that the ratio of the resulting value of liquid water content in the cloudy air case, for $R' = 0.5 \times 10^{-3}\ sec^{-1}$, to the adiabatic value is 0.85, at time t = 11.5 min.

Therefore, a reduction of the adiabatic values of the liquid water content by 10-15%, with the drop concentration remaining the same, simulates roughly the entrainment process with cloudy air.

This might be a simpler way by which the cloudy air entrainment process can be included in a more complicated model.

CHAPTER 5

SUMMARY

In this study an attempt is made to investigate the single effect of entrainment of environmental air into a growing cloud core on the development of the droplet spectrum.

The model described by Leighton and Rogers (1974) is used to determine the droplet spectrum evolution by condensation and coalescence.

Three cases are examined, one of continental cloud and two of maritime cloud. The initial distributions have been chosen to be representative of continental and maritime droplet spectra respectively.

The entrainment rate parameters used are 10^{-3} sec^{-1} and 0.5×10^{-3} sec^{-1}. The vertical velocities have been considered constant at 10 m sec^{-1} for the continental cloud case and 2.5 m sec^{-1} for the maritime cloud case. The assumption of a uniform vertical velocity of the rising cloud parcel is not realistic. Nevertheless by including entrainment in the model, under the same assumptions, a relative measure of the modification in the development of the droplet spectrum obtained without entrainment was given. Furthermore the fact that the vertical velocity of the rising cloud parcel and the entrainment rate parameter are kept constant with height is not consistent from a dynamic point of view. However, using the same method a more realistic approach could be made by considering an entrainment rate parameter that varied with height.

The results show that entrainment reduces the temperature and liquid water content of the rising cloud parcel relative to the adiabatic case and especially when entrainment with clear air is considered. Also as the entrainment rate parameter increases this reduction becomes larger.

Furthermore entrainment does not influence very much the droplets that have grown by condensation, but slows down the production of large drops, especially for entrainment with clear air. In particular entrainment with clear air slows down the development of the droplet spectrum by approximately 2 minutes, relative to the adiabatic case, for $R' = 10^{-3}\ sec^{-1}$, in the continental case as well as in the maritime cases. As the entrainment rate decreases the time lag of the droplet spectrum development also decreases. Thus the entrainment rate parameter of $0.5 \times 10^{-3}\ sec^{-1}$ applied to the continental cloud case indicates that the delay of the development in the clear air case is approximately 1 min.

On the other hand entrainment with cloudy air delays the development of the droplet spectrum by approximately 100 sec and 50 sec for $R' = 10^{-3}\ sec^{-1}$ and $0.5 \times 10^{-3}\ sec^{-1}$ respectively, for the continental cloud case. For the maritime cloud cases the delay is approximately 1 min, for the value of $R' = 10^{-3}\ sec^{-1}$.

Therefore, entrainment of cloud with its environmental air delays the formation of rain, as was expected. However this delay does not seem to be very significant, if it is considered from the point of view of the time lag, in particular when entrainment with cloudy or saturated air takes place.

It should be mentioned that clear air entrainment as has been modeled in this study is an oversimplification. This is because clear air contains cloud condensation nuclei that will be activated as they are mixed in to the core of the cloud, a factor that has not been considered. Furthermore entrainment with cloudy air (containing small droplets) is not equivalent to the process of entrainment with clear air containing CCN. But proceeding in this way an indication of the effect of smaller droplets on the development of the spectrum was obtained.

Finally from the intermediate assumption of entrainment with saturated clear air we obtained results very similar to those of entrainment with cloudy air.

This similarity is an indication of the minor effect of the entrained small droplets. In the case of entrainment with saturated clear air as well as in the case of entrainment with cloudy air the same amount of condensation takes place. The position of the condensation peak is slightly shifted to larger radii in the clear saturated air case. Despite that, the coalescence tail shows a slightly slower development compared to the cloudy air case. This may be attributed to the fact that in the case of cloudy air, the entrained small droplets speed up somewhat the coalescence process by broadening the condensation peak, relative to the quite narrow peak appearing in the saturated clear air case.

On the other hand the only difference between the cases of entrainment of clear saturated air and of clear unsaturated air is in the amount of condensation. The fact that in the case of saturated clear air the development is faster than in the case of unsaturated clear air indicates the importance of the combination of condensation along with coalescence, on the development of the droplet spectrum, as shown by Leighton and Rogers.

Thus the results provide an estimate of the magnitude of the effect of entrainment on the droplet growth, and furthermore an indication of the effect of small droplets on the development of the droplet spectrum.

Finally the simulation of entrainment in the adiabatic model indicates that by just reducing the adiabatic values of the water content by 10-15%, the cloudy or saturated air entrainment can be roughly approximated.

REFERENCES

Árnason, G., and R.S. Greenfield, 1971: Micro- and macro-structures of numerical simulated convective clouds. J. Atmos. Sci., 29, pp. 256-261.

Battan, L.J., and C.H. Reitan, (1957): Droplet size measurements in convective clouds. In Artifical Stimulation of Rain, ed. H. Weickmann and W. Smith (London: Pergamon Press), p. 184.

Beard, K.V., and H.R. Pruppacher, 1969: A determination of the terminal velocity and drag of small water drops by means of a wind tunnel. J. Atmos. Sci., 24, pp. 1066-1072.

Berry, E.X., 1967: Cloud droplet growth by coalescence. J. Atmos. Sci., 24, pp. 688-701.

Byers, H.R., and E.C. Hull, 1949: Inflow patterns of thunderstorms as shown by winds aloft. Bull. Amer. Met. Soc., 30, pp. 90-96.

Danielsen, E.F., R. Bleck and D.A. Morris, 1972: Hail growth by stochastic collection in a cumulus model. J. Atmos. Sci., 29, pp. 135-155.

Diem, M., 1948: Messungen der Grösse von Wolkenelementen. II. Met. Rdsch. I, 261 pp.

English, M., 1973: Alberta hailstorms part II. Growth of large hail in the storm. Meteorology Monographs., Vol. 14, No. 36.

Haltiner, G.J., 1959: On the theory of convective currents. Tellus., 11, pp. 4-15.

Hocking, L.M., and P.R. Jonas, 1970: The collision efficiency of small drops. Quart. J. Roy. Met. Soc., 96, pp. 722-729.

Houghton, H.G., and H.E. Crammer, 1951: A theory of entrainment in convective currents. J. Meteor., 8, pp. 95-102.

Itier, B., 1972: Etude de l'entrainement dans les nuages convectifs. Part of Ph.D. thesis, University of Clermont Ferrand.

Johnson, D.S., 1957: Trade wind cloud measurements windward of the island of Hawaii. Tellus., 9, pp. 495-508.

Kovetz, A., 1969: An analytical solution for the change of cloud and fog droplet spectra due to condensation. J. Atmos. Sci., 26, pp. 302-304.

------, and B. Olund, 1969: The effect of coalescence and condensation on rain formation in a cloud of finite vertical extent. J. Atmos. Sci., 26, pp. 1060-1065.

Lavoie, R.L., 1967: Background data for the warm rain project. Tellus., 19, pp. 348-353.

Leighton, H.G., and R.R. Rogers, 1974: Droplet growth by condensation and coalescence in a strong updraft. J. Atmos. Sci., 31, pp. 271-279.

Malkus, J.S., 1954: Some results of a trade-cumulus cloud investigation. J. Meteor., 11, pp. 220-237.

Mason, B.J., 1971: The Physics of Clouds. Clarendon Press, Oxford, p. 580.

Mason, B.J., and P.R. Jonas, 1974: The evolution of droplet spectra and large droplets by condensation in cumulus clouds. Quart. J. Roy. Met. Soc., 100, pp. 23-38.

Nelson, L.D., 1971: A numerical study on the initiation of warm rain. J. Atmos. Sci., 28, pp. 752-762.

Reinhardt, R.L., 1972: An analysis of improved numerical solutions to the stochastic collection equation for cloud droplets. Ph.D. thesis, University of Nevada, 111 pp.

Ricou, F.P., and D.B. Spalding, 1961: Measurements of entrainment by axisymmetrical turbulent jets. J. Fluid. Mech., 11, pp. 21-32.

Rogers, R.R., 1967: Doppler radar investigation of Hawaiian rain. Tellus., 19, pp. 432-455.

Rogers, R.R., and J.E. Jiusto, 1966: An investigation of rain on the island of Hawaii. CAL. No. VC-2049-P-1. Cornell Aeronautical Laboratory.

Saunders, P.M., 1961: An observational study of cumulus. J. Meteor., 18, pp. 451-467.

Scott, W.T., 1968a: Analytic studies of cloud droplet coalescence I. J. Atmos. Sci., 25, pp. 54-65.

Shafrir, U., and M. Neiburger, 1963: Collision efficiencies of two spheres falling in a viscous medium. J. Geophys. Res., 68, pp. 4141-4147.

Silverman, B.A., and M. Glass, 1973: A numerical simulation of warm cumulus clouds: part I. Parameterized vs nonparameterized microphysics. J. Atmos. Sci., 30, pp. 1620-1637.

Squires, P., 1956: The micro-structure of cumuli in maritime and continental air. Tellus., 8, pp. 443-444.

Squires, P. 1958a: The microstructure and colloidal stability of warm clouds. I. The relation between structure and stability. Tellus. 10, p. 256.

Squires, P., and J.S. Turner, 1962: An entraining jet model for cumulonimbus updraughts. Tellus., 14, pp.422-434.

Squires, P., and J. Warner, 1956: Some measurements in the orographic cloud of the island of Hawaii and in trade wind cumuli. Tellus., 9, pp. 475-494.

Srivastava, R.C., 1964: A model of convection with entrainment and precipitation. Ph.D. thesis, McGill University, 111 pp.

Stommel, H., 1947: Entrainment of air into a cumulus cloud. J. Meteor., 4, pp. 91-94.

Turner, J.S., 1963: Model experiments relating to thermals with increasing buoyancy. Quart. J. Roy. Met. Soc., 89, pp. 62-74.

Warner, J., 1955: The water content of cumuliform cloud. Tellus., 7, p. 449.

Warner, J., 1969: The microstructure of cumulus cloud. Part I. General features of the droplet spectrum. J. Atmos. Sci., 26, pp. 1049-1059.

------, 1969: The microstructure of cumulus cloud. Part II. The effect on droplet size distribution of the cloud nucleus spectrum and updraft velocity. J. Atmos. Sci., 26, pp. 1272-1282.

------, 1970a: The microstructure of cumulus cloud. Part III. The nature of the updraft. J. Atmos. Sci., 27, pp. 682-688.

------, 1970b: On steady-state one-dimensional models of cumulus convection. J. Atmos. Sci., 27, pp. 1035-1040.

------, 1972: The microstructure of cumulus cloud. Part IV. The effect on the droplet spectrum of mixing between cloud and environment. J. Atmos. Sci., 30, pp. 256-261.

Zaitsev, V.A., 1950: Liquid water content and distribution of drops in cumulus clouds. Trudy Glanvoi Geofiz, Obs. No. 19(81), p. 122. Trans. Nat. Res. Council of Canada TT395.

APPENDIX 1.

Computer Program for the Thermodynamic Procedure

For the calculations of the thermodynamic properties of the rising cloud parcel experiencing entrainment, a computer program has been written. This program was adapted to each case of entrainment (clear, cloudy, or saturated) with some slight modifications. It consists of a main program, four subroutines and five functions.

The subroutines, INTER and MIXPSE, have been written to accomplish the problem of entrainment. The other subroutines and functions were taken from a computer program written by N. Cherry.*

The computer program of entrainment with cloudy air for an entrainment rate parameter 10^{-3} sec^{-1}, is given below. The applied initial and environmental conditions are those of the continental case.

MAIN PROGRAM

Input data.

1. Vertical velocity of the rising cloud parcel (V)
2. Potential temperature at the cloud base (THETAD)
3. Saturation mixing ratio at the cloud base (Ws)
4. Temperature at the cloud base (Tc)
5. Minimum height from the cloud base where the calculations start (Hmin)
6. Time interval of calculations, in seconds (ΔT)
7. Total number of time steps that the calculations carried out (NT)
8. Initial value of liquid water content at Hmin

-- Subroutine, INTER, interpolates ambient temperature and dew point soundings

---

*McGill University
Unpublished work

— Subroutine, HTOP, calculates the pressure at each height.

-- Subroutine, FIND, calculates the temperature and saturation mixing ratio of the rising pseudoadiabatically cloud parcel, when equivalent potential temperature (THE), and the pressure (P), are known.

-- Subroutine, MIXPSE, carries out the three steps of mixing, namely pseudoadiabatic ascent, isobaric mixing, wet-bulb process.

Function, Es, calculates the saturation vapor pressure over the water.

Function, Tw, calculates the wet-pulb temperature.

Function, Ws, calculates the saturation mixing ratio.

Function, THAE, calculates the equivalent potential temperature.

Function, THD, calculates the potential temperature.

Output:

At each time step (i.e. height) the following properties were obtained: Pressure, temperature, saturation mixing ratio, density, and liquid water content of the cloud parcel. These parameters are subsequently used as input data for the computer program (Appendix 2) which determines the droplet spectrum development.

```
C
C      MAIN PROGRAM
C
       DIMENSION PR(901),TM(901),WM(901),T(901),TD(901),DENSTY(901),
      1AML(901),AML2(901),RM(901),TX(10),TDX(10),NX(9),NDX(9)
       DATA TX/280.4,273.,263.,261.,261.,253.,227.4/,NX/88,115,50,36,
      1112,309/
       DATA TDX/280.4,273.,263.,261.,261.,253.,227.4/,NDX/88,115,50,36,
      1112,309/
     1 TIMB=0.
       READ(5,10,END=600) V,THETAD,WS,TC,HMIN,AML1,DT,NT
       WRITE(6,60) V,THETAD,WS,TC,HMIN,AML1,DT,NT
    60 FORMAT(' ',7F12.3,I6)
       NTX=NT+1
       J1=6
       L=NT
       T(1)=280.4
       CALL INTER(TX,NX,T,J1,L)
       J2=6
       K=NT
       TD(1)=280.4
       CALL INTER(TDY,NDX,TD,J2,L)
       THETA=THETAD*EXP((597.3*WS)/(0.2396*TC))
       CALL HTOP(P,HMIN,0.,1)
       WRITE(6,63) P
    63 FORMAT(' P=',F10.2)
       CALL FIND(THETA,P,TH,W)
       WRITE(6,64) TH
    64 FORMAT(' TH=',F10.2)
       AML(1)=AML1*(1./(0.348*(P/TH)*1000.))
       WRITE(6,67) AML(1)
    67 FORMAT(' AML=',E15.6)
       DO 6 I=1,NTX
     6 RM(I)=0.001
       DO 500 I=1,NT
       H=HMIN+V*TIMB
       CALL HTOP(P,H,0.,1)
       PR(I)=P
       AML2(I)=AML1*(1./(0.348*(PR(I)/T(I))*1000.))
   500 TIME=TIME+DT
       I2=NT
       CALL MIXPSE(THETA,PR,T,TD,RM,TM,WM,1,I2,AML,AML2)
       TIME=0.
       DO 550 I=1,NT
       TV=TM(I)*(1.0+0.622*WM(L))
       DENSTY(I)=0.348*PR(I)/TV
   550 TIME=TIME+DT
       PUNCH 13,(PR(I),TM(I),WM(I),DENSTY(I),AML(I),I=1,NT)
    13 FORMAT(5E14.5)
       WRITE(6,12)
    12 FORMAT(1H,2X,'I',8X,'P',12X,'TM',13X,'WM',13X,'D',13X,'AML',13X,'
      1AML2')
       WRITE(6,11) (I,PR(I),TM(I),WM(I),DENSTY(I),AML(I),AML2(I),I=1,NT)
    11 FORMAT(I5,6E14.5)
    10 FORMAT(7F10.1,I5)
   600 STOP
       END
C
```

```
      SUBROUTINE INTER(TX,N,T,J,L)
C
      DIMENSION T(1),TX(1),N(1)
      I3=0
      DO 20 K=1,J
      I2=N(K)
      DO 10 I=2,I2
      I4=I+I3
      T(I4)=((TX(K+1)-TX(K))*(I-1))/(N(K)-1)+TX(K)
   10 CONTINUE
      I3=I3+N(K)-1
   20 CONTINUE
      RETURN
      END
C
      SUBROUTINE HTOP (P,H,DP,M)
C
C
      H=H/1000.
      IF (H    .GT.3.0) GO TO 2
      P    =1013.0*EXP(-0.122*H)
      GO TO 4
    2 IF (H    .GT.9.0) GO TO 3
      P    =700.7*EXP((3.0-H    )/7.228)
      GO TO 4
    3 P    =305.6*EXP(-0.1564*(H    -9.0))
    4 P    =P    +DP
    1 CONTINUE
      H=H*1000.
      RETURN
      END
C
      SUBROUTINE MIXPSE(THE,P,T,TD,R,TM,WM,J1,J2,AML,AML2)
C
      DIMENSION P(1),T(1),TD(1),R(1),TM(1),WM(1),AML(1),AML2(1)
      CP=0.2396
      CPV=0.441
      THED=THE
      CALL FIND (THED,P(J1),TM(J1),WM(J1))
      JS=J1+1
      DO 1 J=JS,J2
      CALL FIND(THED,P(J),TM(J),WM(J))
      W=WS(P(J),TD(J))
      AML(J)=AML(J-1)+(WM(J-1)-WM(J))
      TM(J)=(CP*(TM(J)+R(J)*T(J))+CPV*(WM(J)*TM(J)+R(J)*W*T(J))+
     1(AML(J)*TM(J)+AML2(J)*T(J)*R(J)))/(CP*(1.0+R(J))+CPV*(WM(J)+
     2R(J)*W)+(AML(J)+R(J)*AML2(J)))
      AML(J)=(AML(J)+R(J)*AML2(J))/(1.0+R(J))
      WM(J)=(WM(J)+R(J)*W)/(1.0+R(J))
      W1=WM(J)
      TM(J)=TW(P(J),TM(J),WM(J),AML(J))
      WM(J)=WS(P(J),TM(J))
```

```
      AML(J)=AML(J)-(WM(J)-WI)
    1 THED=THAE(P(J),TM(J),WM(J))
      WRITE(6,48) THED
   48 FORMAT(' ',5F10.2)
      RETURN
      END
C
      SUBROUTINE FIND(THE,P,T,Q)
C
      AL=597.3
      R=0.068557
      CP=0.2396
      AK=R/CP
      ERR=0.01
      ER=0.01*ERR
      T0=140.0
      DT=100.
      E=ES(T0)
      Q=0.62197*E/(P-E)
      TEST2=THE-T0*7.211*EXP(AL*Q/(CP*T0))/(P**AK)
      T=T0
      GO TO 2
 1    T=T-DT
      DT=0.1*DT
      IF (DT.LT.ER ) GO TO 5
      E=ES(T)
      Q=0.62197*E/(P-E)
      RKS=AK*(1.0+1.608*Q)/(1.0+0.4652*Q/CP)
      THD=T*((1000.0/(P-E))**RKS)
      TEST2=THE-THD *EXP(AL*Q /(CP*T))
 2    T=T+DT
      E=ES(T)
      Q=0.62197*E/(P-E)
      RKS=AK*(1.0+1.608*Q)/(1.0+0.4652*Q/CP)
      THD=T*((1000.0/(P-E))**RKS)
      TEST1=THE-THD *EXP(AL*Q /(CP*T))
      IF (ABS(TEST1).LT.ERR) GO TO 10
      FACT=TEST1*TEST2
      IF (FACT.LE.0.0) GO TO 1
      TEST2=TEST1
      GO TO 2
 5    WRITE (6,6) P
 6    FORMAT (' ',10X,'T AT P = ',F7.1,' NOT FOUND')
 10   RETURN
      END
C
      FUNCTION ES(T)
C
C     ES(MB) = SATN. VAPOUR PRESSURE OVER WATER AT T(K). W.M.O.,164(13)
C
      TT=373.16/T
      A=-7.90298*(TT-1.0)
      B=5.02808*ALOG10(TT)
      C2=(1.0-1.0/TT)*11.344
      C1=10.0**C2-1.0
      C=-1.3816*C1/10**7
      D2=(1.0-TT)*3.49149
      D1=10.0**D2-1.0
```

```
      D=8.1328*D1/10.0**3
      E=ALOG10(1013.246)
      FF=A+B+C+D+E
      ES=10.0**FF
      RETURN
      END
C
      FUNCTION TW(P,T,W,AML)
C
      AL=597.3
      C=0.2396+W*0.441+AML
      OS=WS(P,T)
      IF(W.EQ.OS) GO TO 3
      DT=0.05
      IF(W.LT.OS) DT=-0.05
      TW=T
      R1=(W-OS)*AL
    1 TW=TW+DT
      IF(TW.GT.350.0.OR.TW.LT.150.0) GO TO 4
      OS=WS(P,TW)
      R2=(W-OS)*AL-(TW-T)*C
      TEST=R1*R2
      IF(TEST.LE.0.0) GO TO 2
      R1=R2
      GO TO 1
    2 TW=TW-R2*DT/(R2-R1)
      RETURN
    3 TW=T
      RETURN
    4 TW=T
      WRITE(6,5)
    5 FORMAT('0',10X,'TW WAS NOT FOUND SO TW=T .',/)
      RETURN
      END
C
      FUNCTION WS(P,T)
C
      WS=0.62197*ES(T)/(P-ES(T))
      RETURN
      END
C
      FUNCTION THAE(P,T,W)
C
      CP=0.2396
      AL=597.3
      THAE=THD(P,T,W)*EXP(AL*W/(CP*T))
      RETURN
      END
C
      FUNCTION THD(P,T,W)
C
      AK=0.28613105
      AKS=AK*(1.0+1.608*W)/(1.0+1.941569*W)
      E=W*P/(0.62197+W)
      THD=T*((1000.0/(P-E))**AKS)
      RETURN
      END
```

APPENDIX 2.

Cloud Droplet Growth Model

Some slight modifications have been made to the model of Leighton and Rogers (1974) to include entrainment. The program given below is for the case of entrainment with cloudy air (containing small droplets), for an entrainment rate parameter 10^{-3} sec^{-1} .

MAIN PROGRAM

Input data.

1. Time interval, in seconds, for integration of coalescence and condensation equations. (DT)
2. Time interval at which complete spectra are printed out. (NP)
3. Initial distribution taken at Hmin. (Number of drops/m^3/unit interval of J).
4. All the input and output parameters of the thermodynamic procedure.
5. The main program reads also the values of collection Kernel (V(I,J)), found in a separate program.

Output.

At each time step the program calculates the spectrum and its corresponding parameters, such as liquid water content, droplet concentration, radius of the 100th largest drop m^{-3}, reflectivity factor.

Details can be found in Reinhardt's (1972) thesis.

```
      DIMENSION F2(85),G2(85)
      COMMON /AREA1/ F(85),G(85),GL(85),CG(85),R(85),X(85),ZJ,XZ,TIME,
     1CX,JMAX,JMIN
      COMMON /AREA2/ SLIC(85,6),TLIC(85,2),CGLFIN(85),AINT(85),WGI
      COMMON /AREA3/ V(87,87)
      COMMON/AREA4/PR(900),TV(900),W(900),DENSTY(900),AML(900),C1
      COMMON/AREA5/WZ,UINT,VOL,RAIN,VLIG,AML1
      ETA(X)=(171.3+0.5575*X)*1.0E-06
      VBIG=0.
      READ (5,12) DT,NP
12    FORMAT (F10.1,I2)
      CX=SQRT(1.414214)
      PI=3.14159
      RZ=3.94E-4
      R(1)=RZ
      X(1)=4.1887* RZ**3
      XZ=X(1)
      ZJ=12./ALOG(2.)
      ZJ3=ZJ/3.
      CR= XP(1./ZJ)
      JMAX=81
      JMIN=1
      JSUP=JMAX+4
      DO 104 J=2,JSUP
      R(J)=CR R(J-1)
104   X(J)=CX X(J-1)
101   READ (5,11, ND=2000) (F(J)    ,J=1,55)
11    FORMAT (5E15.5)
      DO 102 J=56,JMAX
      F(J)  -0.
      G(J)=0.
102   DG(J)-0.
      READ (5,13) VV,THETAC,WS,TC,HMIN
13     FORMAT (5F10.4)
      THE  =THETAD+EXP((597.3*WS)/(0.2396*TC))
      WRITE (6,10) VV,THETAD,WS,TC,HMIN,THE
10    FORMAT (1H1,'V -',F8.2,'    THETAD =',F8.2,'    WS =',F8.2,'    TC ='
     1,F8.2,'    HMIN -',F8.2,'THETAE =',F8.2)
      READ (5,46) NT
46    FORMAT (I5)
      READ(5,50) P,TVV,WZ,C1,AML1
   50 FORMAT(5E14.5)
      JL=1
      N=NT-1
      NT2=NT/2
      READ(5,50) (PR(IT),TV(IT),W(IT),DENSTY(IT),AML(IT),IT=1,N)
      TEMP=TVV-273.
      VISC=ETA(TEMP)
      U=WZ
      TIME=0.
      VOL=0.
      Z=0.
      DROPS=0.
      ICON=1
      H=HMIN
      DO 150 J=1,55
      F(J)=F(J)*1.E08
      G(J)=X(J)*ZJ*F(J)
```

```
 150  DG(J)=0.
      DO 160 J=1,JMAX
      F2(J)=F(J)
  160 G2(J)=G(J)
C
      CALL COLPH
C
C     INITIALIZE SPECTRUM AND LWC
C
      DO 20 J=JMIN,JSUP
      IF (G(J)-1.E-70) 30,30,19
 19   GL(J)=ALOG(G(J))
 20   AINT(J)=G(J)
 30   JM=J-1
      DO 40 I=J,JSUP
      F(I)=0.
      DG(I)=0.
      GL(I)=-180.
 40   G(I)=0.
 210  CALL TRAPIN(DGP,JM)
      VOL=DGP/ZJ
      BINT=VOL/(D1 1000.)
      DO 220 J=1,JM
 220  AINT(J)=X(J)*G(J)
      CALL TRAPIN(DGP,JM)
      Z=36.E+6/(5.869604*ZJ)*DGP
      Z10=10. ALOG10(Z)
      DO 225 J=1,JM
 225  AINT(J)=F(J)
      CALL TRAPIN(DGP,JM)
      DROPS=DGP
      WRITE(6,25) TIME,H,P,D1,TVV,Q,ANL1
 25   FORMAT (1H0,'TIME=',F8.2,'HEIGHT=',F8.1,'PRESSURE=',F8.1,'DENSITY=
     1',F8.4,'VIRT. TEMP.=',F8.1,'SAT. MIX.RATIO=',E12.3,'ANL=',E12.3,//
     2)
      WRITE (6,26)
 26   FORMAT (1H0,3X,'J',13X,'R',19X,'X',19X,'F',18X,'GX',18X,'DG')
      WRITE (6,32) (J,R(J),X(J),F(J),G(J),DG(J),J=1,JMAX)
 32   FORMAT (I5,5E20.6)
      CALL D10C(J100)
      WRITE (6,35) VOL,DROPS,J100,Z10
 35   FORMAT (1H ,'CONCENTRATIONS/UNIT VOL  ARE',E15.4,' G/M**3',E15.4,
     1'DROPS/M**3','      100 TH DROP IS IN CATEGORY',I3,
     2/'      Z=  ',F10.2,' DB')
      READ (10,70) ((V(I,J),I=1,87),J=1,87)
 70   FORMAT (20A4)
      DO 1000 IT=1,N
      I5=70
      TIME TIME+DT
      H-HNIN+WV*TIME
      IF (IT.EQ.1) GO TO 228
      DR=DENSTY(IT)/DENSTY(IT-1)
      GO TO 229
 228  DR=DENSTY(IT)/D1
 229  CONTINUE
      ADR=ALOG(DR)
      EAR=DENSTY(IT)/D1
      JMIN-1
```

```
      DO 235 J=JMIN,JM
      F(J)=(1000./1001.)*F(J)*DR+(1./1001.)*F2(J)*CAR
      G(J)=F(J)*X(J)*ZJ
      VBIG VECTOR
  235 GL(J)=ALOG(G(J))
C
C     CALCULATE CHANGE IN SPECTRUM
C
 260  CALL SPCFB(JM)
C
C     CALCULATE NEW SPECTRUM AND LWC
C
      IA=JM+4
      DO 290 J=JMIN,IA
      G(J)=G(J)+DG(J)*DT*(1.1946/DENSTY(IT))**0.3
      F(J)=G(J)/(X(J)*ZJ)
      IF (G(J)-1.E-70) 270,270,280
 270  G(J)=0.
      F(J)=0.
      DG(J)=0.
      GL(J)=-180.
      GO TO 292
 280  GL(J)=ALOG(G(J))
 290  AINT(J)=G(J)
      JM=IA
      GO TO 293
 292  JM=J-1
 293  IF (JM.LE.JMAX) GO TO 295
      IA=JMAX+1
      DO 294 J=IA,JM
      G(J)=0.
      F(J)=0.
      DG(J)=0.
      GL(J)=-180.
 294  CONTINUE
      JM=JMAX
 295  CALL TRAPIN(DGP,JM)
      VOL=DGP/ZJ
 291  DO 281 J=JMIN,JM
 281  AINT(J)=G(J)/X(J)
      CALL TRAPIN(DGP,JM)
      Z=36.E+6/(S.369004*ZJ)*DGP
      ZIO=10.*ALOG10(Z)
      DO 282 J=JMIN,JM
 282   AINT(J)=F(J)
      CALL TRAPIN(DGP,JM)
      DROPS=DGP
      CALL DIDE(JL30)
C
C     OUTPUT LWC AND NEW SPECTRUM
C
  355 WRITE(6,26) TIME,H,FH(IT),DENSTY(IT),TV(IT),W(IT),AWL(IT)
      IF (MOD(IT,NP)) 360,360,370
 360  WRITE (6,33)
      WRITE (6,32) (J,R(J),F(J),G(J),GL(J),DG(J),J=1,JM)
 33   FORMAT (1H),3X,'J',13X,'R',14X,'F',15X,'G',18X,'GL',18X,'DG')
 370  WRITE (6,35) VOL,DROPS,J100,Z10
      IF (ISW.EQ.1) GO TO 1000
```

```
      CALL CON(IT,JM,1)
      IS=1
      GO TO 271
 1000 CONTINUE
 2000  CALL EXIT
      END
      SUBROUTINE CON(IT,JM,NI)
      COMMON /AREA1/ F(85),C(85),GL(85),DG(85),R(85),X(85),ZJ,XZ,TIME,
     1CX,JMAX,JMIN
      COMMON /AREA2/ GLIC(85,6),TLIC(85,2),COEFIN(85),AINT(85),WGI
      COMMON /AREA3/ V(87,87)
      COMMON/AREA4/PI(900),IV(900),W(900),DENSTY(900),AML(900),C1
      COMMON/AREA5/WZ,BINT,VOL,RAIN,VBIG,AML1
      C1(X)=(X**5+5.*X**3+5.*X**2)-(5.*X**4+6.*X)
      C2(X)=(X**5+16.*X**2)-(4.*X**4+X**3+12.*X)
      C3(X)=(X**5+15.*X**2+4.*X)-(3.*X**4+5.*X**3+12.)
      C4(X)=(X**5+8.*X**2+12.*X)-(2.*X**4+7.*X**3)
      C5(X)=(X**5+X**2+6.*X)-(X**4+7.*X**3)
      C6(X)=(X**5+4.*X)-(3.*X**3)
      RZ=3.94E-4
      IOK=0
      JU=JM
      NIT=1
      WRITE (6,102)
  102 FORMAT (1H0,3X,'TIME',7X,'NIT',3X,'JL',5X,'TRAT',8X,'BINT',8X,
     1'PTEST',8X,'TCT')
      TRAT=AML(IT)-AML1
      JL=JMIN
      PTEST=(VOL+VBIG)/(DENSTY(IT)*1000.)-BINT-TRAT
      IF (PTEST.LE.0.) GO TO 800
      JMIN=JL+NI
      TCT=0.
  205 WRITE(6,101) TIME,NIT,JMIN,TRAT,BINT,PTEST,TCT
  101 FORMAT(1X,E12.4,2I5,4E12.4)
      IF (NIT.GE.16) GO TO 550
      TCT=R(JMIN)**2-R(JL)**2
      IF ((R(JM)**2+TCT).GT.R(JM+1)**2) JU=JM+1
      DO 401 JRO=JMIN,JL
      RO =R(JRO)
      IF (JRO.GT.JMIN) GO TO 210
      RA=R(JL)
      GC=G(JL)
      GO TO 400
  210 RA=SQRT(RO*RO-TCT)
      FJR=1.+ZJ*ALOG(RA/RZ)
      J1=INT(FJR)
      P=FJR-J1
      IF (J1.LE.3) GO TO 250
      DO 220 K=1,6
      IF (GL(J1-3+K).LT.-174.) GO TO 250
  220 CONTINUE
      GC=-C1(P)*GL(J1-2)/120.+C2(P)*GL(J1-1)/24.-C3(P)*GL(J1)/12.+C4(P)*
     1GL(J1+1)/12.-C5(P)*GL(J1+2)/24.+C6(P)*GL(J1+3)/120.
      GO TO 260
  250 CONTINUE
  251 GC=(1.-P)*GL(J1)+P*GL(J1+1)
  260 CONTINUE
      GC=EXP(GC)
```

```
400   DG(JRO)=(RO/RA)**5*GC
401   CONTINUE
      DO 410 J=JMIN,JU
410   AINT(J)=DG(J)
      CALL TRAPIN(DGP,JU)
      TINT=DGP/ZJ
      IF (IOK.EQ.1) GO TO 600
      RAT=(TINT+VOIG)/(DENSTY(IT)*1000.)-BINT
      TEST=RAT-THAT
      IF (TEST) 420,600,430
420   JMIN=JMIN+NI
      NIT=NIT+1
      PTEST=TEST
      GO TO 205
 430  IF(ABS(TEST)-ABS(PTEST)) 600,600,425
425   IF(NIT.GT.1) GO TO 467
      JMIN=JL
      GO TO 800
467   IOK=1
      JMIN=JMIN-NI
      PTEST=TEST
      GO TO 205
590   WRITE (6,100)
100   FORMAT (' TCT SEARCH FAILED')
      CALL EXIT
 600  WRITE(6,101)  TIME,NIT,JMIN,THAT,TINT,PTEST,TCT
      JM=JU
      DO 700 J=JMIN,JM
      G(J)=DG(J)
      GL(J)=ALOG(G(J))
      DG(J)=0.
700   F(J)=G(J)/(X(J)*ZJ)
      IF ((JMIN-JL).LE.0 ) GO TO 730
      JM1=JMIN-1
      DO 720 J=JL ,JM1
      DG(J)=0.
      G(J)=0.
      F(J)=0.
720   GL(J)=-180.
730   CONTINUE
      VOL=TINT
      IF (JM-JMAX)    750,750,740
740   JM=JMAX
      G(JU)=0.
      F(JU)=0.
      DG(JU)=0.
      GL(JU)=-180.
750   CONTINUE
      RETURN
800   TCT=0.
      WRITE(6 101)  TIME,NIT,JMIN,THAT,BINT,PTEST,TCT
      WRITE (6,105)
105   FORMAT (' NO CONDENSATION THIS STEP')
      RETURN
      END
      SUBROUTINE SPCHG(JM)
      COMMON //REAL/ F(85),G(85),GL(85),DG(85),R(85),X(85),ZJ,XZ,TIME,
     1CA,JMAX,JMIN
```

```
      COMMON /AREA2/ GLIC(85,6),TLIC(85,2),COEFIN(85),AINT(85),WGI
      COMMON /AREA3/ V(87,87)
      COMMON/AREA4/PR(900),TV(900),W(900),DENSTY(900),[illegible](900),C1
      AZJ=ALOG(ZJ)
C
C     REGION ONE--LOSS ONLY
C
      J4=JMIN+4
      J5=JMIN+5
      DO 920 J=JMIN,J4
      DO 900 JP=JMIN,J
 900  AINT(JP)=G(JP)* V(JP,J)
      M=J+1
      DO 901 JP=M,JM
 901  AINT(JP)=G(JP)*  V(J,JP)
      CALL INTEGL(DGM,J,JM)
      IF (DGM.LE.0.) GO TO 904
      IF ((ALOG(X(J))+GL(J)+ALOG(DGM)-AZJ).GT.-179.) GO TO 910
 904  DG(J)=0.
      GO TO 920
 910  DG(J)=-X(J)*G(J)*DGM/ZJ
 920  CONTINUE
C
C      REGION TWO -- GAIN AND LOSS
C
      IF (JMIN.GT.1) GO TO 35
 20   GC=EXP(TLIC(5,1)*GL(2)+TLIC(5,2)*GL(3))
      DGP=0.5 X(6)*G(1)*  V(6,1)                    *GC/(X(6)-X(1))
      DO 980 JP=JMIN,J
 980  AINT(JP)=G(JP)* V(JP,6)
      M=J+1
      DO 981 JP=M,JM
 981  AINT(JP)=G(JP)*  V(6,JP)
 30   CALL INTEGL(DGM,6,JM)
      DG(6)-X(6)*(DGP-G(6)*DGM)/ZJ
      J5=JMIN+6
 35   DO 1020 J=J5,JM
      JO-J-4
      AINT(JO)=0.
      M=JO-1
      DO 990 JP=JMIN,M
      CALL INTERP(J,JP)
      IF ((ALOG(WGI)+ALOG(G(JP))).GT.-179.) GO TO S8S
      AINT(JP)=0.
      GO TO 990
 989  AINT(JP)=WGI*G(JP)*(X(J)/(X(J)-X(JP)))
 990  CONTINUE
      IF (JMIN.NE.4) GO TO 4C
      DGP=0.5 AINT(JP)
      GO TO 45
 40   CALL INTEGG(DGP,JO)
      M=J-1
 45   DO 1000 JP=JMIN,M
 1000 AINT(JP)=G(JP)* V(JP,J )
      DO 1002 JP=J,JM
 1002 AINT(JP)=G(JP)* V(J,JP),
 50   CALL INTEGL(DGM,J,JM)
      DG(J)=     X(J)*(DGP-G(J)*DGM)/ZJ
```

```
 1020 CONTINUE
C
C      REGION THREE -- GAIN ONLY
C
       IF(JM.GE.JMAX) GO TO 1041
       IA=JM+1
       IB=J+4
       IF (IB.GE.JMAX) IB=JMAX
       DO 1040 J=IA,IB
       JD=J-4
       AINT(JD)=0.
       M=JD-1
       DO 1030 JP=JMIN,M
       CALL INTERP(J,JP)
       IF (WGI.LE.0.) GO TO 1028
       IF ((GL(JP)+ALOG(WGI)).GT.-179.) GO TO 1029
 1028  AINT(JP)=0.
       GO TO 1030
 1029  AINT(JP)=X(J)/(X(J)-X(JP))*WGI*G(JP)
 1030  CONTINUE
 60    CALL INTEGG (DGP,JD)
 1035  IF (DGP.LE.0.) GO TO 1036
       IF ((ALOG(DGP)+ALOG(X(J))-A2J).GT.-179.) GO TO 1039
 1036  DG(J)=0.
       GO TO 1040
 1039  DG(J)=     X(J)*DGP/ZJ
 1040  CONTINUE
 1041  CONTINUE
       RETURN
       END
       SUBROUTINE COLPD
       COMMON /AREA1/ F(85),G(85),GL(85),DG(85),R(85),X(85),ZJ,XZ,TIME,
      1CA,JMAX,JMIN
       COMMON /AREA2/ SLIC(85,6),TLIC(85,2),COEFIN(85),AINT(85),WCI
       COMMON /AREA3/ V(87,87)
       COMMON/AREA4/PR(900),TV(900),W(900),DENSTY(900),ANL(900),CI
C
C      SIX POINT AND TWO POINT LAGRANGE INTERPOLATION COEFFICIENTS
C
       CC=4./.6931718
       DO 500 I=1,4
       TLIC(I,1)=0.
       TLIC(I,2)=0.
       DO 500 J=1,5
 500   SLIC(I,J)=0.
       DO 540 I=5,45
       CI=CX**(-I)
       IF (CI-0.01) 510,510,520
 510   D=5.-9.*CI/6.
       D=4.-4.*CI/3
       D=3.-4.*CI/3
       D=2.-CI/6
       D=1.-CI/6
       A=-CC*CI/D
       GO TO 530
 520   A=CC*ALOG(1.-CI)
 530   A5=A**5
       A4=A**4
```

```
      A3=A**3
      A2=A*A
      J=I-4
      GO TO (532,534,534,530,536,536),J
      SLIC(I,1)=(-A5-4.*A+5.*A3)/120.
      SLIC(I,2)=(A4-7.*A3+(A5-A2 +6.*A))/24.
      SLIC(I,3)=(-A5+1.*A2 -12.*A-(2.*A4-7.*A3)))/12.
      SLIC(I,4)=(3.*A4-5.*A3+12.+(A5-1.)*A2 +4.*A))/12.
      SLIC(I,5) (-A5+16.*A2 -(4.*A4-A3-12.*A))/24.
      SLIC(I,6)=(5.*A4-6.*A+(A5+5.*A3-5.*A2 ))/120.
      TLIC(I,2)=A+1.
      TLIC(I,1)=-A
      GO TO 540
  532 SLIC(5,1) =-((A5+85.*A3+274.*A)+(15.*A4+225.*A2+120.))/120.
      SLIC(5,2)=((A5+95.*A3+324.*A)+(16.*A4+260.*A2+144.))/24.
      SLIC(5,3)=-((A5+107.*A3+396.*A)+(17.*A4+307.*A2+180.))/12.
      SLIC(5,4)=((A5+121.*A3+508.*A)+(18.*A4+372.*A2+240.))/12.
      SLIC(5,5)=-((A5+137.*A3+702.*A)+(19.*A4+461.*A2+360.))/24.
      SLIC(5,6)=((A5+155.*A3+1044.*A)+(20.*A4+580.*A2+720.))/120.
      TLIC(5,1)=-A-3.
      TLIC(5,2)=A+4.
      GO TO 540
  534 SLIC(I,1)=-((A5+35.*A3+24.*A)+(10.*A4+50.*A2)) /120.
      SLIC(I,2)=((A5+41.*A3+30.*A)+(11.*A4+61.*A2))/24.
      SLIC(I,3)=-((A5+49.*A3+40.*A)+(12.*A4+78.*A2))/12.
      SLIC(I,4)=((A5+59.*A3+60.*A)+(13.*A4+107.*A2))/12.
      SLIC(I,5)=-((A5+71.*A3+120.*A)+(14.*A4+154.*A2))/24.
      SLIC(I,6)=((A5+85.*A3+274.*A)+(15.*A4+225.*A2+120.))/120.
      TLIC(I,1)=-A-2.
      TLIC(I,2)=A+3.
      GO TO 540
  536 SLIC(I,1)=-((A5+5.*A3-5.*A2)+(5.*A4-6.*A))/120.
      SLIC(I,2)=((A5+7.*A3-6.*A2)+(6.*A4-8.*A))/24.
      SLIC(I,3)=-((A5+11.*A3-7.*A2)+(7.*A4-12.*A))/12.
      SLIC(I,4)=((A5+17.*A3-2.*A2)+(8.*A4-24.*A))/12.
      SLIC(I,5)=-((A5+25.*A3-24.)+(9.*A4-25.*A+15.*A2))/24.
      SLIC(I,6)=((A5+35.*A3+24.*A)+(10.*A4+50.*A2))/120.
      TLIC(I,1)=-A-1.
      TLIC(I,2)=A+2.
  540 CONTINUE
C
C     THREE POINT LAGRANGE INTEGRATION COEFFICIENTS
C
      DO 550 L=1,42
      COEFIN(2*L-1)=2.
  550 COEFIN(2*L)=4.
      RETURN
      END
      SUBROUTINE INTEGG(EGF,JQ)
      COMMON /AREA1/ F(85),G(85),GL(85),CG(85),R(85),X(85),ZJ,X2,TIME,
     1CX,JMAX,JMIN
      COMMON /AREA2/ SLIC(85,6),TLIC(85,2),COEFIN(85),AINT(85),EGI
     * COMMON /AREA3/ V(87,87)
      COMMON/AREA4/PH(900),TV(900),W(900),DENSTY(900),AML(900),CI
      IF (JQ-JMIN-2) 2960,2980,2990
 2960 DGP=0.
      DO 2970 IA=JMIN,JQ
 2970 DGP=DGP+.5*AINT(IA)
```

```
      GO TO 3060
 2980 DGP=(AINT(JMIN)+4.*AINT(JMIN+1)+AINT(JMIN+2))/3.
      GO TO 3060
 2990 DGPT=0.
      JT=JO-JMIN+1
      JL=JT/2
      IF (JT-2*JL) 3000,3010,3000
 3000 DGP=7.*AINT(JO)+32.*AINT(JO-1)+12.*AINT(JO-2)+32.*AINT(JO-3)+7.*AI
     1NT(JO-4)
      DGP=2.*DGP/45.
      IB=JO-5
      GO TO 3020
 3010 DGP=3.*AINT(JO)+9.*AINT(JO-1)+9.*AINT(JO-2)+3.*AINT(JO-3)
      DGP=DGP/8.
      IB=JO-4
 3020 IF (JT-5) 3050,3050,3030
 3030 DGPT=AINT(JMIN)+AINT(IB+1)
      K=JMIN+1
      IF (MOD(JMIN,2).EQ.1) GO TO 3035
      DO 3032 IA=K,IB
 3032 DGPT=DGPT+COEFIN(IA+1)*AINT(IA)
      GO TO 3050
 3035 DO 3040 IA=K,IB
 3040 DGPT=DGPT+COEFIN(IA)*AINT(IA)
 3050 DGP=DGP+DGPT/3.
 3060 RETURN
      END
      SUBROUTINE INTEGL (DGM,LA,LB)
      COMMON /AREA1/ F(85),C(85),GL(85),DG(85),R(85),X(85),ZJ,XZ,TIME,
     1CX,JMAX,JMIN
      COMMON /AREA2/ SLIC(85,6),TLIC(85,2),COEFIN(85),AINT(85),NGI
      COMMON /AREA3/ V(87,87)
      COMMON/AREA4/PR(900),TV(900),W(900),DENSTY(900),ANL(900),CI
      ID=0
      IE=0
      IF (MOD(JMIN,2).EQ.0) IE=1
      IF (MOD(LA,2).EQ.1) IC=1
      LT=LA-JMIN+1
      IF (LT-3) 4000,4020,4030
 4000 DGM=0.
      DO 4010 IA=JMIN,LA
 4010 DGM=DGM+.5*AINT(IA)
      GO TO 4130
 4020 DGM=(AINT(JMIN)+4.*AINT(JMIN+1))/3.
      GO TO 4130
 4030 DGMT=0.
      KA=LT/2
      IF (LT-2*KA) 4040,4050,4040
 4040 CONTINUE
      DGM=32.*AINT(LA-1)+12.*AINT(LA-2)+32.*AINT(LA-3)+7.*AINT(LA-4)
      DGM=DGM*2./45.
      IB=LA-5
      GO TO 4060
 4050 CONTINUE
      DGM=(9.*AINT(LA-1)+9.*AINT(LA-2)+3.*AINT(LA-3))/8.
      IB=LA-4
 4060 IF (LT-5) 4090,4090,4070
 4070 DGMT=AINT(JMIN)+AINT(IB+1)
```

```
      JMI 41-JMIN+1
      DO 4030 IA=JMIN1,IE
4080  DGMT=DGMT+COEFIN(IA+IE)*AINT(IA)
4090  DGM=DGM+DGMT/3.
      IF (LB-LA-2) 4100,4120,4130
4100  DO 4110 IA=LA,LB
4110  DGM=DGM+.5*AINT(IA)
      GO TO 4180
4120  DGM=DGM+(AINT(LB)+4.*AINT(LB-1))/3.
      GO TO 4180
4130  DGM=DGM+(3.*AINT(LA+1)+9.*AINT(LA+2)+3.*AINT(LA+3))/8.
      IF (LB-LA-5) 4140,4160,4160
4140  IB=LA+3
      DO 4150 IA=IB,LB
4150  DGM=DGM+.5*AINT(IA)
      GO TO 4180
4160  DGMT=AINT(LA+3)+AINT(LB)
      IB=LA+4
      IC=LB-1
      DO 4170 IA=IB,IC
4170  DGMT=DGMT+COEFIN(IA+IC)*AINT(IA)
      DGM=DGM+DGMT/3.
4180  RETURN
      END
      SUBROUTINE INTERP (J,JP)
      COMMON /AREA1/ F(85),G(85),GL(85),DG(85),R(85),X(85),ZJ,XZ,TIME,
     1CX,JMAX,JMIN
      COMMON /AREA2/ GLIC(85,6),TLIC(85,2),COEFIN(85),AINT(85),WGI
      COMMON /AREA3/ V(87,87)
      COMMON/AREA4/PH(900),TV(900),W(900),DENSTY(900),AML(900),C1
      M=J-JP-4
      GO TO (5001,5002,5002,5003,5003,5003),M
5010  K=4
      L=2
      GO TO 5020
5001  K=7
      L=5
      GO TO 5020
5002  K=6
      L=4
      GO TO 5020
5003  K=5
      L=3
5020  GC=0.
      DO 5030 I=1,6
      IF (GL(J-K+I)+179.) 5050,5050,5030
5030  CONTINUE
      DO 5040 I=1,6
5040  GC=GC+GLIC(J-JP,I)*GL(J-K+I)
      GC=EXP(GC)
      GO TO 5090
5050  DO 5060 I=1,2
5060  GC=GC+TLIC(J-JP,I)*GL(J-L+I)
      GC=EXP(GC)
5090  IF (V(J,JP).LT.1.E-40) GO TO 5091
      TEST=ALOG(GC)+ALOG(V(J,JP))
      IF (TEST.GT.-179.) GO TO 5092
5091  WGI=0.
```

```
      RETURN
 5092 WGI=GC                  * V(J,JP)
      RETURN
      END
      SUBROUTINE J100(J100)
      COMMON /AREA1/ F(85),C(85),GL(85),DG(85),R(85),X(85),ZJ,XZ,TIME,
     1CX,JMAX,JMIN
      JL=JMAX-2
      J100=0
      TO=0.5*(F(JMAX)+F(JL+1))
      DO 60 J=1,JL
      I=JMAX-J
      IF (TO.GE.130.) GO TO 65
   60 TO=TO+(F(I)+F(I-1))*0.5
   61 J100=0
      RETURN
   65 J100=I
      RETURN
      END
      SUBROUTINE TRAPIN(DGF,JQ)
      COMMON /AREA1/ F(85),C(85),GL(85),DG(85),R(85),X(85),ZJ,XZ,TIME,
     1CX,JMAX,JMIN
      COMMON /AREA2/ SLIC(85,6),TLIC(85,2),COEFIN(85),AINT(85),WGI
      DGF=0.5*AINT(JMIN)
      IA=JMIN+1
      DO 3000 J=IA,JQ
      DGF=DGF+AINT(J)
 3000 CONTINUE
      RETURN
      END
```

APPENDIX 3.

The following computer program has been written to provide graphical representation of the droplet spectra obtained by the model, mentioned in the previous Appendix 2.

Plotting Program

MAIN

```
      DIMENSION ZJ(80),G(80)
      REAL WORD(2)
      REAL UNIT(2)
      REAL PARE (1)
      DATA WORD/'RADI','US ('/
      DATA UNIT/'MICR','ONS '/
      DATA PARE/')   '/
      CALL PLOTON
      RSTART=0.
7     CALL PLOT(0.0,2.5,-3)
      CALL DASHY (0.0,0.0,5.0,0.0,1)
      CALL DASHY(0.281,0.0,0.281,-0.062,1)
      CALL DASHY (1.031,0.0,1.031,-0.062,1)
      CALL DASHY (1.781,0.0,1.781,-0.062,1)
      CALL DASHY (2.531,0.0,2.531,-0.062,1)
      CALL DASHY (3.281,0.0,3.281,-0.062,1)
      CALL DASHY (4.031,0.0,4.031,-0.062,1)
      CALL DASHY (4.781,0.0,4.781,-0.062,1)
      CALL NUMBER (0.281,-0.25,0.125,5.,0.,-1)
      CALL NUMBER (0.969,-0.25,0.125,10.,0.,-1)
      CALL NUMBER (1.719,-0.25,0.125,20.,0.,-1)
      CALL NUMBER (2.469,-0.25,0.125,40.,0.,-1)
      CALL NUMBER (3.219,-0.25,0.125,80.,0.,-1)
      CALL NUMBER (3.906,-0.25,0.125,160.,0.,-1)
      CALL NUMBER (4.656,-0.25,0.125,320.,0.,-1)
      CALL SYMBOL(1.75,-0.5,0.125,WORD,0.,8)
      CALL SYMBOL(2.75,-0.5,0.093,UNIT,0.,7)
      CALL SYMBOL(3.401,-0.5,0.125,PARE,0.,1)
      CALL LGAXS(0.0,0.0,'G-AXIS',6,7.0,90.,1.00E-05,1.0)
4     I=0
2     I=I+1
3     READ(5,25,END=1000) ZJ(I),G(I)
25    FORMAT (F5.0,E15.6)
      IF (ZJ(I).EQ.0.) GO TO 1
      IF (ZJ(I).EQ.999.) GO TO 5
      IF (G(I).NE.0.) GO TO 2
      GO TO 3
1     I=I-1
      ZJ(I+1)=1.
      ZJ(I+2)=16.
      G(I+1)=1.0E-05
      G(I+2)=1.0
      CALL LGLIN (ZJ,G,I,1,0,0,1)
      IF (RSTART.EQ.1.) GO TO 6
      GO TO 4
5     RSTART=1.
      GO TO 1
6     CALL PLOT (10.0,-2.5,-3)
      RSTART=0.
      GO TO 7
1000  CALL ENDPLT
      STOP
      END
```